INSTITUTO POLITÉCNICO DE LISBOA

ESCOLA SUPERIOR DE TECNOLOGIA DA SAÚDE DE LISBOA

Patient-derived pancreatic cancer organoids for modeling drug response

Ana Catarina Cardoso Lopes

Supervisor(s): Noélia Maria Fernandes Custódio, Ph.D., Faculdade de Medicina, Universidade de Lisboa
Anita Raquel Quintal Gomes, Ph.D., Escola Superior de Tecnologia da Saúde de Lisboa, Instituto Politécnico de Lisboa

Thesis to obtain the Master of Science Degree in

Tecnologias Moleculares em Saúde

Lisbon 2021

INSTITUTO POLITÉCNICO DE LISBOA

ESCOLA SUPERIOR DE TECNOLOGIA DA SAÚDE DE LISBOA

Patient-derived pancreatic cancer organoids for modeling drug response

Ana Catarina Cardoso Lopes

Supervisor(s): Noélia Maria Fernandes Custódio, Ph.D., Faculdade de Medicina, Universidade de Lisboa
Anita Raquel Quintal Gomes, Ph.D., Escola Superior de Tecnologia da Saúde de Lisboa, Instituto Politécnico de Lisboa

Thesis to obtain the Master of Science Degree in

Tecnologias Moleculares em Saúde

(This version include the jury's suggestions)

Examination Committee

Chairperson: Bruno Filipe Sousa Carmona, Ph.D.
Supervisor: Noélia Maria Fernandes Custódio, Ph.D.
Member of the Committee: Isabel Cristina Ferreira Fernandes Borges da Costa, Ph.D.

Lisbon 2021

Acknowledgments

First, I want to thank Professor Maria do Carmo Fonseca for allowing me to experience the life of a researcher and the chance to grow both professionally and personally at IMM.

A great and special thanks to Doctor Noélia Custódio, my advisor, who every single day taught me everything she knows and shared her little tricks and tips. She showed me not just the professional she is but the remarkable person as well. In any circumstance made me feel bad about failing or making a mistake. I would particularly like to single out Beatriz Galvão, we together learn the true significance of the expression: “Just believe!”. To them both, thank you for all the nights without sleep, all the weekends we had to work, and all the moments we together laugh. I joined them in this adventure, not knowing much about the organoid world, and they made me feel like I was with them since the beginning, treating the organoids like our babies. I’m incredibly grateful I got to know you, work with you and learn from you during this journey. And thank you also to Catarina Vale for her help.

A special thanks to my internal advisor, Doctor Anita Gomes. Although she had a considerable workload, she never failed to clarify any doubts and advise me on the best way forward. Furthermore, she always responded to my e-mails as soon as I send them.

To the people at Hospital Beatriz Ângelo and Hospital da Luz Lisboa involved in this project, I am grateful because none of the work would have been possible without them. Doctor Marília Cravo, Dr. Catarina Fidalgo, Dr. Luis Mascarenhas-Lemos and Doctor Sandra Faias provided all our tissue samples and performed the histological analysis.

I would also like to thank everyone at Carmo-Fonseca Lab who, from day one, made my expectations grow about the time spent there and made me feel welcome.

My most enormous thanks go to my parents, Jorge Lopes and Maria Cardoso, for their support throughout my life and all the effort they made to make me the person I am and be where I am today. Despite being younger, thanks to my big little brother, Afonso Lopes, for being my example to follow, being my safe haven, and the greatest love of my life. Thanks for putting up with me over the years, especially when I was particularly annoying.

I want to thank my boyfriend, my “chato” André Mateus, for supporting me throughout this adventure and all the reinforce when I was writing this dissertation.

Finally, doing this internship, writing this thesis, and working simultaneously, being a healthcare professional during a world pandemic, was not easy at all. However, this made me grow and learn like I never thought was possible, overcome all the obstacles and be the new person I am today.

Resumo

O adenocarcinoma ductal pancreático é um dos tipos de cancro mais letais, com uma taxa de sobrevivência de cinco anos abaixo de 10%, para o qual há uma necessidade urgente de novos tratamentos. O único medicamento de precisão aprovado é um inibidor de PARP (PARPi) em tumores com mutação *BRCA*, mas muito poucos doentes beneficiam desta terapia. Recentemente, foram desenvolvidos os inibidores de CDK12/CDK13 (CDK12/CDK13i) que mostraram sensibilizar células tumorais, independentemente de mutações *BRCA*, aos PARPi. Coloca-se então a hipótese que os doentes com PDAC poderiam beneficiar desta terapêutica combinada, independentemente do status mutacional de *BRCA*.

O objetivo principal deste projeto foi investigar se o tratamento com CDK12/CDK13i sensibiliza as células tumorais aos PARPi. Como modelo de estudo, usámos organoides derivados de doentes. Os organoides são culturas primárias tridimensionais que mantêm uma arquitetura celular semelhante ao órgão do qual foram derivadas. Os organoides tumorais recapitulam as características do tumor original e podem prever a sensibilidade à quimioterapia.

No presente estudo, as amostras de tecido foram obtidas de doentes submetidos a resseção cirúrgica ou biópsia por agulha fina. Foram obtidas seis linhas de organoides tumorais, caracterizadas por coloração com hematoxilina e eosina e imunofluorescência. Foi testada a sensibilidade aos fármacos carboplatina, PARPi olaparib, CDK12/CDK13i SR-4835 e a combinação de olaparib com SR-4835. Os organoides tumorais testados não são sensíveis à carboplatina, mas são sensíveis ao SR-4835. A resposta ao olaparib é dependente do paciente, com apenas uma linha sensível. A combinação de olaparib com SR-4835 é sinérgica em todos os casos, exceto no caso sensível ao olaparib.

Palavras-chave: organoides, CDK12, medicina de precisão, adenocarcinoma ductal pancreático, resposta a fármacos.

Abstract

Pancreatic ductal adenocarcinoma (PDAC) is one of the deadliest types of cancer, with a five-year survival rate below 10%, for which there is an urgent need for new treatments. The only approved precision drug is a PARP inhibitor (PARPi) in tumors with *BRCA* mutation, but very few patients benefit from this therapy. Recently, CDK12/CDK13 inhibitors (CDK12/CDK13i) were developed and shown to sensitize cancer cells devoid of *BRCA* mutations to PARPi. We hypothesized that patients with PDAC could benefit from this combination therapy irrespective of their *BRCA* mutational status.

This project's main objective was to investigate whether treatment with CDK12/CDK13i sensitizes pancreatic cancer cells to PARPi. As a model system, we used patient-derived organoids. Organoids are three-dimensional primary cultures that maintain a cell architecture resembling the organ from which they were derived. Tumor organoids recapitulate the characteristics of the original tumor and can predict its sensitivity to chemotherapy.

In the present study, tissue samples were obtained from patients undergoing surgical resection or fine-needle biopsy. Six PDAC organoid lines were obtained, characterized by hematoxylin and eosin staining and immunofluorescence. Their sensitivity to the drugs carboplatin, PARPi olaparib, CDK12/CDK13i SR-4835, and the combination of olaparib with SR-4835 were tested. The PDAC organoids tested are not sensitive to carboplatin but are sensitive to SR-4835. The response to olaparib is patient-dependent, with only one PDAC organoid line being sensitive. The combination of olaparib with SR-4835 is synergistic in all the cases, except for the one sensitive to olaparib.

Keywords: cancer organoids, CDK12, precision medicine, pancreatic ductal adenocarcinoma, drug response.

Contents

List of Figures

Glossary

2D	Two-dimensional
3D	Three-dimensional
ASCO	American Society of Clinical Oncology
BM	Basal culture Medium
BRCA	BReast CAncer gene
BSA	Bovine Serum Albumin
CAF	Cancer-Associated Fibroblasts
CDK12/CDK13i	Cyclin-Dependent Kinase 12 and Cyclin-Dependent Kinase 13 inhibitor
CDK12	Cyclin-Dependent Kinase 12
CDK13	Cyclin-Dependent Kinase 13
CDK	Cyclin-Dependent Kinase
CI	Combination Index
CRISPR/Cas9	Clustered Regularly Interspaced Short Palindromic Repeats associated protein 9
CTD	Carboxy-Terminal Domain
DAPI	4',6'-DiAmino-2-Phenil-Indol
DDR	DNA Damage Repair
DMEM	Dulbecco's Modified Eagle Medium
DMSO	DiMethyl SulfOxide
DPBS	Dulbecco's Phosphate-Buffered Saline
DSB	Double-Strand Breaks
ECM	ExtraCellular Matrix
EGF	Epidermal Growth Factor
EMA	European Medicines Agency
EpCAM	Epithelial Cell Adhesion Molecule

FBS	Fetal Bovine Serum
FDA	United States Food and Drug Administration
FNA	Fine-Needle Aspiration
FNB	Fine-Needle Biopsy
HR	Homologous Recombination
H&E	Hematoxylin and Eosin
IC_{50}	Half-maximal inhibitory concentration
OS	Overall Survival
PARPi	Poly (Adenosine diphosphate-Ribose) Polymerase inhibitors
PARP	Poly (Adenosine diphosphate-Ribose) Polymerase
PBS	Phosphate-Buffered Saline
PC	Pancreatic Cancer
PDAC	Pancreatic Ductal AdenoCarcinoma
PDO	Patient-Derived Organoids
PDX	Patient-Derived Xenograft
PFA	ParaFormAldehyde
SSB	Single-Strand Breaks
TGF-β	Transforming Growth Factor β
cDNA	complementary DeoxyriboNucleic Acid
iPSCs	induced Pluripotent Stem Cells

1 Introduction

Pancreatic ductal adenocarcinoma (PDAC) is a deadly disease, being the most common type of pancreatic cancer [1]. Currently, the average survival rate at five years is three to nine percent in Portugal [1, 2]. Symptoms can be difficult to identify because generally they are vague and unspecific, making recognition and early diagnosis difficult. The high mortality due to the late manifestation of this type of cancer highlights the need for early detection methods and new treatment strategies, such as new combinations of drugs. Precision medicine approaches are emerging, as well as new methods for testing those approaches, such as the newly developed organoid technology. Organoids are currently used to study targeted drug therapies because they maintain the gene expression profiles of primitive tumors [3–5]. This chapter will provide an overview of previous research and related work on this topic.

1.1 Pancreatic Cancer

Pancreatic cancer (PC) is the digestive system's malignant tumor with the worst prognosis [1, 6]. In fact, PC has the lowest survival rate of all cancers in Europe and already constitutes the third cause of death by cancer [6, 7]. Its incidence is in progression and is estimated to represent the second cause of cancer-related death in western countries by 2030 [8, 9]. It was the fourth cancer with more estimated deaths in the United States in 2020 [10].

In Portugal, PC is the third most common neoplasm of the digestive system after colon and stomach cancer [1]. There are 1619 cases each year, corresponding to 2.8% of all cancers [2]. There is a higher prevalence in males, with highest overall mortality between ages 75-79 [1, 2]. The expectation of life at diagnosis is only 4.6 months, and the number of deaths from PC has almost doubled in the past three decades [1, 2]. There are several types of pancreatic tumors, however, adenocarcinoma is the most common (95%) [1, 11].

Symptoms depend on the tumor location and can be challenging to identify because they are generally vague and unspecific (including jaundice, light-colored stools, abdominal pain, weight loss and fatigue [9]), making recognition and early diagnosis difficult [12, 13]. Up to 2% of PC cases are thought to be related to genetic conditions [14]. Family history is found in

5–10% of patients, with PDAC occurring mainly in families with ovarian or breast cancers [15].

1.1.1 Classification and diagnosis

About 90% of PCs start in the exocrine cells that delimit the pancreatic channels (Figure 1.1). This type of cancer is called ductal adenocarcinoma [2, 12]. Another type of tumor, less frequent, is neuroendocrine carcinoma that originates in the pancreas' endocrine cells. Pancreatic cancer in the form of sarcoma or lymphoma is less frequent [2]. Approximately 60% of cancers occur in the head of the pancreas, close to the duodenum, 20% occur in the body and tail of the pancreas, and the remainder are diffuse tumors [2].

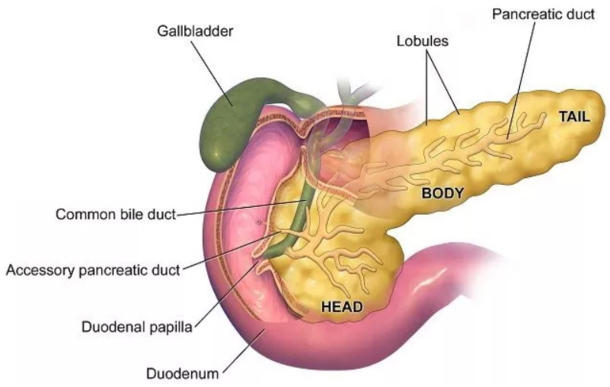

Figure 1.1: **Pancreas Anatomy.** The pancreas is located behind the stomach being among the most important digestive organs. It secretes enzymes, involved in the digestion of carbohydrates, fats, and proteins [16].

The cellular origins of human PDAC are not yet totally understood. Germline mutations in various cancer susceptibility genes have been implicated in the pathogenesis of PDAC. These include dysregulation of *KRAS*, *CDKN2A*, *TP53* and *SMAD4*, but also *BRCA1*, *BRCA2*, *PALB2*, *ATM* and the mismatch repair genes [8, 17–20]. Driehuis et al. [21] identified *KRAS* as the most commonly altered gene (88%) in PDAC patient-derived organoids (PDOs), and detected mutations in *BRAF* and *NRAS*. *TP53* was mutated or lost in 84% of PDOs and loss of *CDKN2A* was detected in 80%. Other commonly found genetic alterations included loss of *SMAD4*, *EEF2A* mutations, *MYC* amplifications, activating mutations in *PIK3CA*, and *ARID1A* inactivation. There are two main models proposed to describe the development of PDAC. In the "classical" one, acinar-to-ductal metaplasia is followed by acinar-to-ductal reprogramming and the progressive development of pre-neoplastic lesions evolving towards PDAC [8]. The "alternative" pathway has its origin in ductal cells that, through mutations in *GNAS*, *KRAS*, *TP53* and *RNF43*, form cystic lesions secreting mucin, with intraductal papillary mucinous neoplasia or mucinous cystic neoplasia being the most implicated in progression to PDAC [8]. Iqbal et al. [18] found a statistically significant increase in the incidence of PC in female *BRCA* mutation

carriers and observed a poor overall survival (OS) in both men and women with a *BRCA1* or *BRCA2* mutation.

There are three subtypes identified for PDAC being classical, quasimesenchymal, and exocrine-like, given the subtype-specific gene expression, according to Collison et al. [22, 23]. The classical subtype has a high expression of epithelial and adhesion-associated genes, the quasimesenchymal shows high expression of mesenchyme-associated genes, and the exocrine-like shows relatively high expression of tumor cell–derived digestive enzyme genes [8, 22]. The classical subtype is characterized by differentiated duct cell marker expression and favorable prognosis, whereas the quasimesenchymal is characterized by aggressive clinical behavior [19]. The work of Matsushita et al. [24] demonstrated that clones from single cells were capable of differentiating into both microvilli and stereocilia coated cells, supporting the concept of bi-phenotypic differentiation of PDAC.

Diagnosis of PDAC is often late as the symptoms appear at an advanced stage of the disease. CA19-9 remains one of the best biomarkers for assessing PDAC progression but is not specific enough to be used for early detection [25]. On the other hand, the pancreas has a deep location in the abdomen, with many surrounding structures, making it difficult to observe all its segments with an imaging method [6, 26]. When symptoms are already present, an abdominal ultrasound is usually sufficient for the cancer diagnosis. Computed tomography, magnetic resonance and echoendoscopy are usually necessary to confirm the diagnosis and tumor staging [6]. Suspicious lesions are typically diagnosed via endoscopic ultrasound-guided fine-needle aspiration (FNA) or biopsy [27, 28]. At the time of diagnosis, only 10-20% of patients are surgical candidates and, for those, survival at 5 years is only 15-30% [6, 8, 12, 29]. In recent years, we have witnessed important progress in research to find molecular biomarkers that allow a therapy aimed at new targets which can have an impact on the prognosis of the disease.

PC remains one of the most lethal. Between 2010 and 2014, the global survival rates were 5-15%, with Portugal registering 10.7% [1]. Survival after PDAC resection has been linked with many factors, including grade and stage, but no factor has been consistently prognostic [22, 26]. One study [30] found that 76% of recurrences occur at a distant site, demonstrating that most patients with PDAC have a systemic disease at the time of resection. Almost 20% of the patients who were free of recurrence after five years developed disease recurrence. This study established that distinctive clinicopathological features correlate with different patterns of recurrence. The impact of biomarkers on diagnosis or identifying risk groups can be decisive in changing this paradigm.

1.1.2 Treatment

The gold standard for patients with resectable PC is upfront resection followed by adjuvant chemotherapy [12]. For those patients who are ineligible for surgical resection, palliative chemotherapy is usually performed, but the median OS for these patients is less than one year [12, 19]. There is the possibility of neoadjuvant chemotherapy that nowadays in PDAC is shifting from tumor shrinkage to controlling potential micrometastases and selecting patients who may benefit from radical resection [31].

The standard-of-care treatments are the combination chemotherapy regimens Gemcitabine/nab-Paclitaxel or FOLFIRINOX (5-Fluorouracil, Irinotecan and Oxaliplatin) [8, 12] each with an approximately 30% response rate [32] and with a significant average increase of survival of up to one year [8]. However, these treatment concepts do not consider tumor heterogeneity such as specific genetic alterations, mutational burden, expression pattern, or stroma composition such as mesenchymal and immune cells [33]. Different approaches have been tested in phase III trials to improve outcomes with combination therapy, but few have been successful [12].

Gemcitabine [34] is a pyrimidine antimetabolite, converted intracellularly by nucleotide kinases into diphosphate and triphosphate. The cytotoxic action of gemcitabine is due to DNA synthesis inhibition through a double diphosphate and triphosphate action. After its incorporation into DNA, gemcitabine appears to induce the programmed process of cell destruction known as apoptosis. It is approved by European Medicines Agency (EMA) for advanced local or metastatic pancreatic adenocarcinoma [34].

Nab-paclitaxel [35] is a formulation of paclitaxel attached to a protein - albumin - that affects how the medicine works in the body and is approved for metastatic adenocarcinoma of the pancreas, as the first treatment in combination with gemcitabine. Paclitaxel is an antimicrotubular agent that promotes microtubules' union from tubulin dimers and stabilizes the microtubules avoiding depolymerization. This stability results in inhibition of the normal dynamic reorganization of the microtubule network, which is essential for mitotic and interphase functions. Nab-paclitaxel contains nanoparticles of paclitaxel-albumin, which quickly dissociate into complexes of soluble paclitaxel bound to albumin. Albumin promotes the transport of paclitaxel through endothelial cells [35].

5-Fluorouracil is an analog of uracil, a ribonucleic acid component, thought to act as an antimetabolite. After intracellular conversion in the active deoxynucleotide, it interferes with DNA synthesis. It can also interfere with RNA synthesis [36]. Irinotecan is a semi-synthetic derivative of camptothecin that acts as a specific inhibitor of DNA topoisomerase I. The inhibition of DNA topoisomerase I by Irinotecan induces single-strand lesions in DNA that blocks the

DNA replication fork and is responsible for cytotoxicity [37]. Oxaliplatin is a platinum-derived compound whose aqueous derivatives, resulting from biotransformation, interact with DNA and form cross-links, resulting in an interruption in DNA synthesis leading to cytotoxic and antitumor effects [38]. FOLFIRINOX regimen is recommended as the standard for metastatic pancreatic cancer by the National Comprehensive Cancer Network, American Society of Clinical Oncology (ASCO), and European Society for Medical Oncology [12]. In *BRCA*-associated cancers, with appropriate family history, platin-based chemotherapy such as FOLFIRINOX should be preferred because mutations in the *BRCA* genes are known to increase the sensitivity of pancreatic cancers towards platin due to the lack of an efficient DNA repair system [39].

Precision medicine approaches to treating PDAC are emerging. Namely, tumors that harbor mutations in genes related to double-strand DNA repair such as *BRCA1* or *BRCA2* (incidence varying between 5-10% [14]) have been associated with better responses to platinum-based chemotherapy agents [40], such as carboplatin. However, tumors that harbor mutations in essential genes can utilize the Poly (ADP-ribose) polymerase (PARP) pathway as a salvage repair mechanism. Therefore, PARP inhibition could lead to tumor destruction and synthetic lethality in presence of *BRCA* mutations [14, 40]. Indeed, various PARP inhibitors (PARPi) have been approved for the treatment of patients with germline or somatic *BRCA* mutant breast, and ovarian cancer [40]. PARPi exerts their cytotoxic effects through a synthetic lethal pathway (Figure 1.2), thereby killing tumor cells with defects in homologous recombination (HR) and/or in the protection of stalled replication forks [14, 15, 41].

Patients with tumors harboring *BRCA1/2* mutations who initially respond to PARPi eventually develop drug resistance through multiple mechanisms, including somatic reversion mutations in *BRCA1/2*, epigenetic reversion of *BRCA1/2* promoter methylation, overexpression of a *BRCA1/2* hypomorph, loss of PARP1 expression, initiation of drug efflux, or acquisition of new mutations in or silencing of other DNA damage repair (DDR) genes such as *REV7*, *EZH2*, and *TP53BP1*. These mechanisms may lead to the restoration of either HR activity or protection of stalled replication forks [3, 41]. Olaparib is the most investigated PARPi and the first agent approved by EMA and United States Food and Drug Administration (FDA). Several PARPi have now also been approved due to level 1 evidence in ovarian cancer, including niraparib and rucaparib [41, 43–45]. However, only olaparib is presently approved for use in advanced PC [46]. PARPi have been assessed as maintenance treatment in frontline and platinum-sensitive recurrence, following response to platinum chemotherapy [41, 47]. Patients with *BRCA*-associated locally advanced PC can benefit from targeted therapy with olaparib as second-line therapy after antimetabolite treatment failure [15]. Olaparib had antitumor activity in a phase 2 trial in

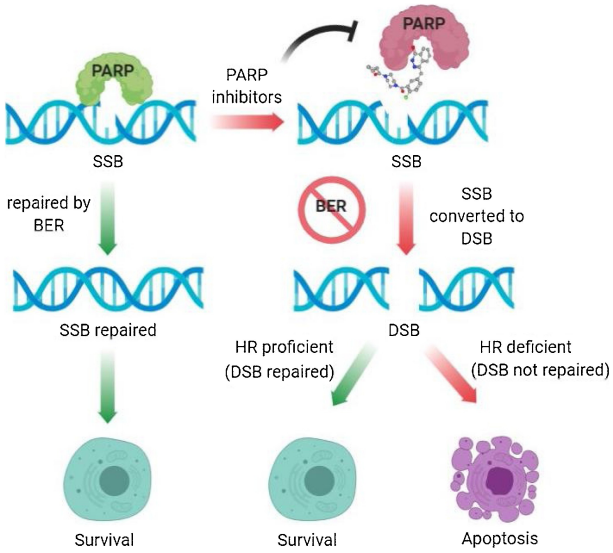

Figure 1.2: **Mechanism of action of PARP inhibitors.** Endogenous single-strand breaks (SSB) occur frequently in proliferating cells, and are repaired mostly by PARP-dependent base excision repair pathway. Efficient repair is essential for the survival of cells. PARP inhibitors inhibit PARP and thus this repair pathway. The unrepaired SSB can be converted to double-strand breaks (DSB) that are toxic to cells, and HR is the major pathway to repair such lesion during cell replication. HR-proficient cells can repair DSB originated from SSB to ensure genome stability and cell survival, while HR-deficient cells that cannot repair those undergo apoptosis and eventually cell death [42].

heavily pretreated patients with a germline *BRCA* mutation and metastatic PC [48]. The indication of olaparib in PC is based on POLO trial that showed a significant progression-free survival benefit with maintenance olaparib to patients with a germline *BRCA* mutation, and metastatic PC that had not progressed during platinum-based chemotherapy [46, 49]. Identifying *BRCA* mutations in patients with PC would provide the opportunity to have personalized therapy with PARPi. Shindo et al. [50] found a significant yield of deleterious germline mutations in PC susceptibility genes in patients with PC without a family history. Although drugs such as PARPi or platinum salts might be an effective treatment strategy for patients with *BRCA1* or *BRCA2* mutations, the selection pressure they provide, driving the emergence of resistant clones with secondary mutations is also profound [51]. Alternative treatment strategies, which suppress or at least delay the emergence of these secondary mutant clones, need to be developed and studied.

1.1.3 CDK12 as a potential therapeutic target

The cyclin-dependent kinase (CDK) family of enzymes engineer the regulation of crucial eukaryotic cellular processes, including the cell cycle and transcription [52]. Transcriptional CDKs phosphorylate the carboxy-terminal domain (CTD) of Rbp1, the largest subunit of RNA Polymerase II, which serves as a platform for recruiting factors controlling transcriptional and post-transcriptional events [53, 54]. Nevertheless, the exact role in transcription regulation or splicing

is not fully understood [54].

Cyclin-dependent kinase 12 (CDK12), a transcriptional CDK with specific roles in regulating transcription of genes involved in cellular responses to stress and DNA damage, was first identified from cDNA screens for cell cycle regulators [52, 53, 55]. In addition to regulating the elongation phase of transcription, CDK12 participates in transcription termination and is involved in splicing. Cyclin-dependent kinase 13 (CDK13) is closely related and shares 43% sequence homology and a mostly conserved kinase domain [55]. CDK12 phosphorylates the CTD of RNA pol II and it is essential for DDR, splicing, and differentiation [4, 54, 56].

The knockdown of CDK12 revealed significantly lower levels of *BRCA1*, *ATR*, *FANCI* and *FANCD2*, leading to genomic instability [57]. CDK12 loss of function can be deployed as a biomarker to select an appropriate therapeutic approach [4, 56]. Using a specific and rapid inhibition of CDK12 kinase activity in analog-sensitive CDK12 cells, Chirackal Manavalan et al. [58] exposed a crucial role for CDK12 catalytic activity in G1/S progression. They showed that CDK12 activity is required for optimal expression of core DNA replication genes and timely formation of the pre-replication complex on chromatin. They further demonstrate that CDK12-dependent RNA Polymerase II processivity is a rate-limiting factor for optimal G1/S progression and cellular proliferation. The group also found that CDK12 inhibition results in transcript shortening for a subset of genes with a higher frequency of poly(A) signals. Lim et al. [59] showed that dinaciclib, a potent inhibitor of CDK12 in combination restored tumor growth inhibition.

Loss-of-function of CDK12 results in decreased HR and enhanced sensitivity to DNA cross-linking agents, such as carboplatin and PARPi [55]. A genome-wide PARPi screen identified CDK12 as a sensitizer to olaparib, and CDK12 mutations were shown to be a possible relevant biomarker of PARPi sensitivity in high-grade serous ovarian cancer [60]. Resistance to PARPi could be overcome by CDK12 inhibition in *BRCA* wild-type and mutated models of triple-negative breast cancer [61]. Synthetic lethal interactions reported for CDK12 with PARPi have led it to grow interest as a biomarker and therapeutic target for response in cancer treatment [52, 55, 62]. CDK12 offers a low-toxicity therapeutic approach because of its multi-functional but context-specific roles in cancer development [56].

SR-4835, an active inhibitor that specifically targets CDK12 and CDK13, which is predicted to compete with ATP binding, completely blocked growth and survival of triple-negative breast cancer cells irrespective of their HR status, with minimal effects on primary cells [52]. It was reported to promote the synergistic effect with DNA damage chemotherapy and PARPi [4]. Importantly, SR-4835 is orally bioavailable and well-tolerated in mice after long-term dosing [52]. CDK12 inhibition is now emerging as a promising strategy for cancer treatment.

1.2 Preclinical models

A better understanding of PC's functional defects is needed to understand which therapies are best suited for each molecular defect and which combinations are least likely to select for resistance. Research for determining precise and sensitive tumor markers for early diagnosis and prognosis evaluation and exploring new strategies, such as targeted therapy and immunotherapy, has risen in the last years [4]. Therefore, preclinical models that can accurately recapitulate the biological characteristics of tumors *in vivo* are essential [4].

The conventional two-dimensional (2D) cell culture has long been established and allows for rapid and reliable growth of cancer cells [63]. Cancer cell lines are easy to culture and can be passaged, cryopreserved, and manipulated both genetically and chemically [29]. However, the major drawback of this technique is that cancer cell lines perform poorly in recapitulating histopathological and molecular phenotype of the original tumor in aspects such as polarity, microenvironment, cell metabolism, and gene expression [8], thereby lacking clinical translatability [5, 19, 64]. During many passages in culture, they can accumulate mutations, potentially leading to positive selection of specific clones without many features of the original tumors [65]. In the case of PC, the efficiency of cell line generation from a resected primary tumor is lower than generating three-dimensional (3D) cultures [29].

Genetically engineered mouse models give an advantage over many other methods to study PDAC because they have native interactions between the stromal and neoplastic cells [29]. Even though these models led to numerous clinical advances in PDAC, they are time-consuming, expensive to breed, and the engineering of additional mutations requires considerable effort. Furthermore, some discoveries in murine models have not been reproduced in humans [29].

Patient-derived xenografts (PDX) are created by transplanting human cancer cells into immunodeficient mice. A more faithful tumor cell environment is created, allowing for a more biological stable tumor model with conserved tumor heterogeneity [63]. They better mimic the original tumor, but their establishment is inefficient, lengthy, and costly, is ethically questionable, and may create mouse-specific tumor evolution [5, 19, 29, 64]. PDXs have been used to find mechanisms of resistance to therapies and biomarkers to predict therapeutic response. However, studies of therapeutic agents' activity on these models found a low correlation with activity in human patients [29].

3D culture methods hold promise to became systems that better mimic the biology found *in vivo*. 3D methods to culture pancreas cells are barely a new phenomenon, having emerged

as part of a larger movement over the last century to be able to culture and study tissues *ex vivo* [29]. 3D culture methods involve embedding cells inside (or culturing cells on top) of a matrix. This matrix provides a physical barrier, preventing cells from attaching and interacting with the culture plate. The matrix also acts as a physical structure with which cells can interact. Collagen and Matrigel are the two most common matrices used for the 3D culture of pancreas cells [29]. Matrigel is a commercial name for a basement membrane extract that is purified from murine Engelbreth-Holm-Swarm tumors [29]. It contains high levels of type IV collagen as well as laminin and enactin/nidogen. When cultured in Matrigel, numerous cell types, including pancreatic cells, have been shown to take on a polarized morphology and have physiologic responses not seen in cells cultured as monolayers [66]. Spheroid is a globular cell aggregate that remains as a floating 3D structure. Compared with cell lines and PDX, spheroids can significantly restore the microenvironment of tumors and maintain similarity to the original tumor [4, 29]. This model requires some caution due to variation in spheroid methods, the propensity for spheroids to aggregate in culture, and quiescent tumor stem cells' potential not to proliferate under spheroid conditions. All may influence the reliability of these assays [29]. Moreover, cell adhesion destruction can quickly induce the dysfunctional apoptosis of epithelial cells and consequently reduce the success rate of globular model culture [4]. Organoids represent *in vitro* self-developing 3D tissue reconstructions, reproducing key features of the tissue of origin [5, 29, 32, 63, 64] and can be derived from embryonic stem or induced pluripotent stem (iPS) cells and primary or tumor tissue [8, 63, 67]. Organoids can be generated from normal tissues, in addition to the tumor tissue, thus solving the problem of no experimental control group caused by spheroids [68]. They appear to be genetically stable over several passages, making them an ideal tool for PDAC modeling and drug testing [8]. They can be cultured from different tissues of different patients, such as primary and metastatic tumors, ascites, pleural effusion drainage, and normal tissue [69–71]. They are faster, easier, and less expensive to generate than PDX [3] and reproduce the morphology, gene expression, cellular metabolic heterogeneity of the primary tumor, and cell polarity [8]. The 3D culture should retain the identity of the modeled organ to be classified as an organoid and contain multiple cell types, preserve some physiological aspects of the organ, and self-organize according to the same principles as the organ. Furthermore, organoids maintain several properties of primary tissues, such as self-renewal, multilineage differentiation and histology [72].

1.3 Patient-derived tumor organoids

Organoid cultures of patient-derived tumors provide an inexpensive and easily manipulable model system for functional assays. They are derived from human stem, or primary tumor cells (typically epithelial cells) that organize into 3D structures anatomically and functionally, mimicking the tumor from which they are derived [3, 4, 73]. They can be long term expanded, can be cryopreserved, and genetically modified, allowing for a wide range of applications in cancer research [5] (Figure 1.3).

PDO culture is now a powerful tool that can be used for precision medicine since it is a simple technique to replicate and can maintain the characteristics of a tumor and its microenvironment *in vivo* [8]. The PDOs maintain homology with primary tumors for a long time. Hence, it is a better model for drug sensitivity screens than cell lines [4, 68].

Tumor-like organs are easy to pass on to form biobanks, which can be used for extensive throughput gene analysis and drug screening [4]. These living biobanks, where organoid cultures representative of disease diversity in terms of pathological subtypes and mutated-gene frequencies, can be stored and disseminated to other researchers [68]. Gene analysis helps uncover disease etiology and find treatment options. Besides being used to examine normal development, PDOs have also been used to study tumorigenesis [68].

PDO cultures may contain immune cells representative of the tumor immune microenvironment, enabling the testing of immune-checkpoint blockade or other immunotherapies, unlike PDX models [3]. Organoids alone cannot generalize the immune system, but researchers have started co-culturing organoids, and lymphocytes [4]. Hans Clevers' team [69, 74] showed that organoids could be established from different tissues of patients, proving that this model recapitulates the heterogeneity of primary tumors. Besides, they showed that organoids could better reflect the sensitivity of tumors to drug treatment regimens.

Overall, PDOs are potentially faithful tumor models that allow for functional testing, prediction of therapeutic sensitivity, and interrogation of specific biomarkers and can be used in PDAC. Large-scale studies of organoids, comparing with patient outcomes, will be required to prove this model system's utility in the clinic and allow new ways for clinical testing. By generating organoids and mimicking the tumor microenvironment, all phases of human cancer progression, including normal cells, preinvasive carcinomas, and invasive and metastatic cells, can be studied in the laboratory and stored in biobanks for worldwide dissemination [68] (Figure 1.3).

1.3.1 Patient-derived pancreatic cancer organoids

Organoids were first developed and used in 2009, for studies in colorectal cancer [26, 63] but in the last years they're use has been growing in other areas such as PDAC [8]. Researchers have been attempting to culture pancreas cells outside the body as far back as 1938 when Carrel and Lindberg were able to keep a cat pancreas alive in culture for four days using a perfusion pump [29]. By the 1980s, numerous methods for culturing the pancreas as organ explants had been reported, and researchers were starting to develop methods for culturing isolated pancreas cells in 3D [29]. Isolation and establishment of organoids were first performed in mice but have progressively been developed in humans to isolate and culture PDAC. The success rate seems highly dependent on the sample's characteristics and the method used [8]. Several studies developed in the last years show that PDOs can be established from PDAC with a success rate of around 70% [21].

Despite tumor cell lines and PDX being the most commonly used human model systems for the study of PC [11, 26, 72], PDOs have now various applications in PDAC, which are depicted in Figure 1.3. They can be derived from primary tumors, either by FNA or true-cut biopsies, with a high rate of success [26] as well as from metastases [8]. FNA or fine-needle biopsy (FNB) material from patients yields intact epithelial cell aggregates and single cells that are mainly free of stromal contamination, as compared with core biopsies that retain acellular matrix [75].

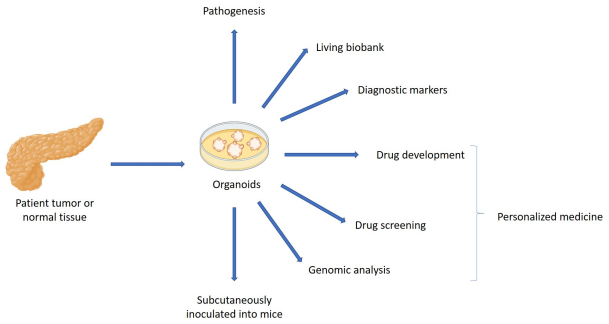

Figure 1.3: **Applications of patient-derived organoids in pancreatic cancer.** Organoids can be used in several areas of cancer research such as pathogenesis and genomic analysis or diagnostic markers. They can produce living biobanks of information for different patients and can also be used to the development of new drugs or to study new drug combinations leading to more personalized medicine.

Ling Huang et al. [17] showed that tumor organoids conserve histological organization, differentiation status, and morphologic heterogeneity observed in primary PDAC, suggesting organoids may be used not only as models for investigating early stages of carcinogenesis but also to predict clinical responses and personalize cancer treatments.

In PDAC, the stroma comprises cancer-associated fibroblasts (CAFs), extracellular matrix (ECM), pancreatic stellate cells, endothelial cells, immune cells, and various growth factors. It

represents up to 90% of the tumor volume and forms a physical barrier preventing drug delivery contributing to drug resistance [8]. For this reason, it is important trying to include these stromal cells in PDOs if possible. Calvin Kuo et al. [76] showed the ability of pancreatic organoids to model the effects of *Kras* mutation alone or in combination with *Trp53* mutation, proving a promising method for studying the steps in tumorigenesis. In addition, stromal cells in these cultures may better mimic tumor-stroma interactions than models where epithelial cells are cultured alone. The ability to genetically engineered organoids efficiently using CRISPR/Cas9 system also enables cancer research [29]. Tsai et al. [77] demonstrated that multi-cell type organotypic co-cultures are a viable technique for the *in vitro* study of PC-associated stromal and immune interactions as well as models of the tumor microenvironment.

If the tumor organoids are cultured individually, the prognosis of patients' tumors can be quickly classified, and their histomorphology and gene expression are detected. Several studies [5, 64, 70, 77, 78] confirmed that the PDO retained histological features of the original tumors. Also, immunostaining for p53 and expression levels of genes resulted in concordant results. Georgakopoulos et al. [79] optimized a human pancreas organoid culture system that enables the long-term expansion of human primary ductal pancreas tissue from both fresh and cryopreserved samples and even as clonal cultures, allowing to maintain the PDO to access the prognosis of patients. They also demonstrated that PDOs maintain chromosome stability and do not transform during long-term engraftment *in vivo*, making them a promising system for disease modeling.

1.3.2 Drug screening and testing

The feasibility and reliability of drug testing based on organoid cultures were first shown in gastrointestinal cancers - with 100% sensitivity, 93% specificity, 88% positive predictive value, and 100% negative predictive value for drug response [8]. PDOs are currently used in the study of targeted drug therapy of various tumors, and those produced from the liver can be employed as a model in testing the candidate drugs against hepatotoxicity [4, 5] (Figure 1.4).

The organoid cultures can be genetically characterized and used for drug screening, which makes it possible to correlate the genetic background of a tumor with drug response [5, 29, 72]. PDOs maintain the gene expression profiles of primitive tumors, as validated by Sarah Hill [3], making it possible to target genes to guide further research on targeted therapy. As they can be cultured on a large scale, this facilitates high-throughput drug screening. Thus, PDO may be useful in rapidly predicting drug combinations' synergy or antagonism in clinical trials and in identifying rational drug-delivery schedules.

The establishment of organoid cultures from the same patient's healthy tissue allows the development of less toxic drugs by screening for compounds that selectively kill tumor cells while leaving healthy cells unharmed (Figure 1.4). In the example of Figure 1.4, drug B seems most suitable for treating this patient because it specifically kills tumor organoids and does not induce hepatotoxicity. Little et al. [80] have used human kidney organoids to illustrate that cisplatin acts as a nephrotoxic.

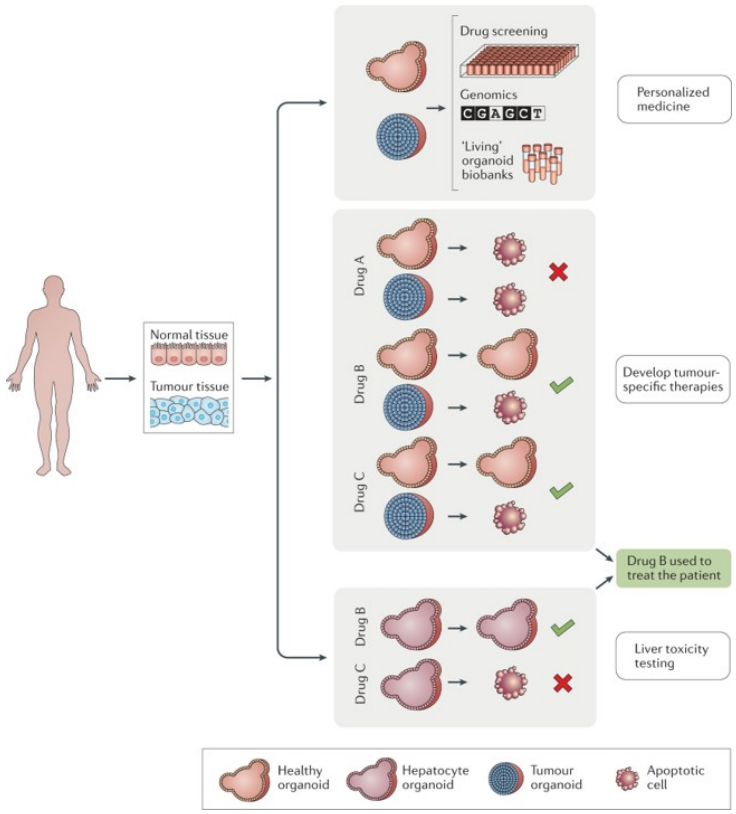

Figure 1.4: **Normal and tumor organoid cultures for drug development and personalized cancer treatment.** Organoids can be established from patient-derived healthy and tumor tissue samples. The organoid cultures can be genetically characterized and used for drug screening, which makes it possible to correlate the genetic background of a tumor with drug response (upper panel). Organoids can be cryopreserved and stored in living organoid biobanks. The establishment of organoids from healthy tissue of the same patient (middle panel) gives the opportunity to develop less toxic drugs by screening for compounds that selectively kill tumor cells while leaving healthy cells unharmed. Self-renewing hepatocyte organoid cultures may be used to test for hepatotoxicity — one of the causes of drug failure in clinical trials — of a potential new drug (lower panel) [5].

A rapid and simple functional assay may be useful in predicting therapeutic sensitivity or resistance. At the time of initial laparoscopic tumor collection, this determination would mandate newer combination therapies up-front in patient treatment and help highlight the therapies that are effective on each patient. This give an advantage for personalized medicine (Figure 1.3). Early studies have revealed multiple examples of exceptional responders to targeted drugs, where expected genetic alterations representing driver oncogenes or synthetic lethal pathways were logically matched to that therapy [29, 68]. Frappart et al. [26] have demonstrated the

feasibility and the predictive nature of PDO in one PDAC patient and may open the possibility of personalized therapeutic management in clinical routine. Tiriac et al. [23] findings suggest that the differential drug responses are related to the co-existence of multiple cancer sub-clones in metastatic patients. This is important to be considered for drug guiding and could explain partial/limited responses observed in some of the patients. Different responses observed for organoids derived from different patients were confirmed by Driehuis et. al [21].

The PDOs also provide models to develop drugs that circumvent innate or acquired resistance. Notably, the relative sensitivity of PDOs to cytotoxic drugs, which have a narrow therapeutic index *in vivo* compared with many targeted agents, may also reflect patients' clinical response to those drugs [68]. Small-scale drug screens on organoid biobanks performed so far have yielded promising results [5, 81]. Studies with larger patient numbers and more extended outcome tracking are required to determine whether organoid testing will be a reliable *in vitro* assay for predicting drug response in the clinic. PDO could also be used for drug testing, streamlining drug companies' efforts for finding new cancer therapies [63]. Developing biobanks of organoids could allow for high throughput drug testing, predicting patient response before administering the therapy. Large biobanks of organoids would allow already developed drugs to be tested *ex vivo*, providing insight into possible resistance mechanisms. Using biobanks from the ideal patient population for a particular drug could also be selected before the clinical trial (Figure 1.4).

Using oncolytic virotherapy is an emerging strategy for treating PDAC, and several viral derivatives are currently being tested in clinical trials. The work of Raimondi et al. [82] is an example of the use of PDOs for this end. They showed that PDOs from PDAC are a promising model for evaluating both selectivity and sensitivity to oncolytic adenoviral therapies. They also demonstrated that adenoviruses can replicate and expand in organoids and that PDOs from individual patients display different sensitivities to oncolytic adenoviruses.

Recently, Schuster et al. [83] developed an automated high-throughput microfluidic platform for culturing pancreatic PDO cultures for continuous monitoring of 3D growth, morphology, and biochemical analysis. Their configuration can create 20 independent experimental conditions, controlled with a second device. Using this platform, they found that combination chemotherapy treatment resulted in significantly increased apoptosis in tumor organoids compared to monotherapy.

Organoids represent one of the most promising tools, contributing for predicting patients' drug response and better delineation of underlying mechanisms of tumor progression.

2 Project goals and contributions

Pancreatic cancer (PC) is a highly lethal malignancy, with a 5-year survival rate of less than 10%. It is currently the fourth leading cause of cancer deaths and is projected to surpass colon and breast cancers by 2030 [29]. The poor outcomes of pancreatic ductal adenocarcinoma (PDAC) patients are due to the late presentation of symptoms which difficult the diagnosis. Also, PDAC tumors have a highly desmoplastic stroma, which forms a stiff, hypoxic tumor mass, rendering therapy ineffective [13]. Researchers need accurate and tractable model systems for studying this malignancy for clinical progress to be made, more specifically in the field of precision medicine.

Tumors that harbor mutations in homologous recombination repair genes can utilize the Poly (ADP-ribose) polymerase (PARP) pathway as a salvage repair mechanism. Therefore, PARP inhibition could lead to tumor destruction and synthetic lethality in presence of *BRCA* mutations [14, 40]. Although drugs such as PARP inhibitors (PARPi) might be an effective treatment strategy for patients with *BRCA* mutation [51], not all PDAC patients can benefit from this therapeutic approach. Alternative treatment strategies need to be developed and studied.

PDAC has been associated with significant levels of aberrations in CDK12 [55] and combining a CDK12/CDK13 inhibitor (SR-4835) with PARPi olaparib, or other DNA-damaging therapeutics was synergistic in triple-negative breast cancer cells [52]. Considering the results of this previous study, we hypothesize that patients with PDAC may benefit from combination therapy with CDK12/CDK13 inhibitors and PARPi (in this case, SR-4835 and olaparib, respectively), regardless of *BRCA* mutations.

Over the last years, various model systems have been established for PDAC, based either on tumor cell lines, genetically engineered mouse models, or xenografts. However, most tumor models fail to mimic tumor heterogeneity and lack the tumor-specific microenvironment that represents a significant impediment for therapeutic response [84]. Recently, organoids have been used to address those issues. In this work, we exploit organoids as a platform to study this malignancy and their use in drug discovery and repositioning. “Drug repositioning” is a promising strategy for drug discovery and development using medicines that have already been

approved for use in humans [85]. The latest data indicates that organoids represent one of the most promising tools, as significant progress was made in predicting patients' drug response and better delineation of underlying mechanisms of tumor progression [84].

Based on everything described so far, the main goal of this project is to investigate whether CDK12/CDK13 inhibition selectively sensitizes PDAC cells to PARPi. The specific objectives are, first, to establish patient-derived cultures of pancreatic ductal organoids as an *ex vivo* assay for precision medicine approaches; second, characterize patient-derived organoids histologically; and last, test drug response of the established organoids to carboplatin, olaparib, and SR-4835 to determine if there is synergy between olaparib and SR-4835 in patient-derived PDAC organoids.

We were able to establish stable lines of organoids from six tumor samples and one normal pancreatic duct sample. With these lines, we found that tumor organoids lack therapeutic sensitivity to carboplatin but are sensitive to SR-4835. The response to olaparib is patient-dependent, with only one PDAC organoid line being sensitive. The combination of olaparib with SR-4835 is synergistic in all the cases, except for the one sensitive to olaparib.

3 Methods

In this chapter we will present the materials and methods used in this project. From patient samples (Section 3.1) to establishing organoid cultures (Section 3.2) and the associated protocols such as decontaminating cultures, organoid freezing and Wnt3a-conditioned medium production (Section 3.3). We show the methods to characterize the organoids, such as histological analysis (Section 3.4) and immunofluorescence microscopy (Section 3.5), and to carry out drug testing (Section 3.6).

3.1 Patient Samples

Tumor samples were obtained from patients undergoing tumor resection surgery and fine-needle biopsy (FNB). The study was approved (Annex I) by the ethical committee of Hospital Beatriz Ângelo (Estudo "HBA nº517 LH nº224", Reference 3391/2020 MJH/CMO/NO), and written consent was obtained from all participants (Annex II). Individual samples were pseudo-anonymized, and only clinicians have access to the medical data.

3.2 Establishing organoid cultures

Small pieces (1–3 cm) of the suspected tumor mass, identified by the surgeon and the pathologist, as well as normal tissue were transported to the laboratory in cold DPBS (grisp; Reference gtc13.0500) and subjected to cell isolation on the same day, within 2 to 3 hours after resection. See images of the received samples on Figure 3.1.

For the generation of pancreatic cancer organoids (Figure 3.2), tissue pieces were washed with ice-cold DPBS, then minced to small fragments in basal medium [Advanced DMEM/F 12 (ThermoFisher; Reference 12634 010), supplemented with 1X GlutaMax (ThermoFisher; Reference 35050-061), 1% (v/v) HEPES (ThermoFisher; Reference 15630-080) and 1% (v/v) Pen-Strep (ThermoFisher; Reference 15070-063)] using a scalpel or scissor. These fragments were poured into pre-warmed ($37^{\circ}C$) basal medium (BM) containing Type II Collagenase (ThermoFisher; Reference 17101-015) to obtain a final concentration of 2.5mg/mL and incubated for

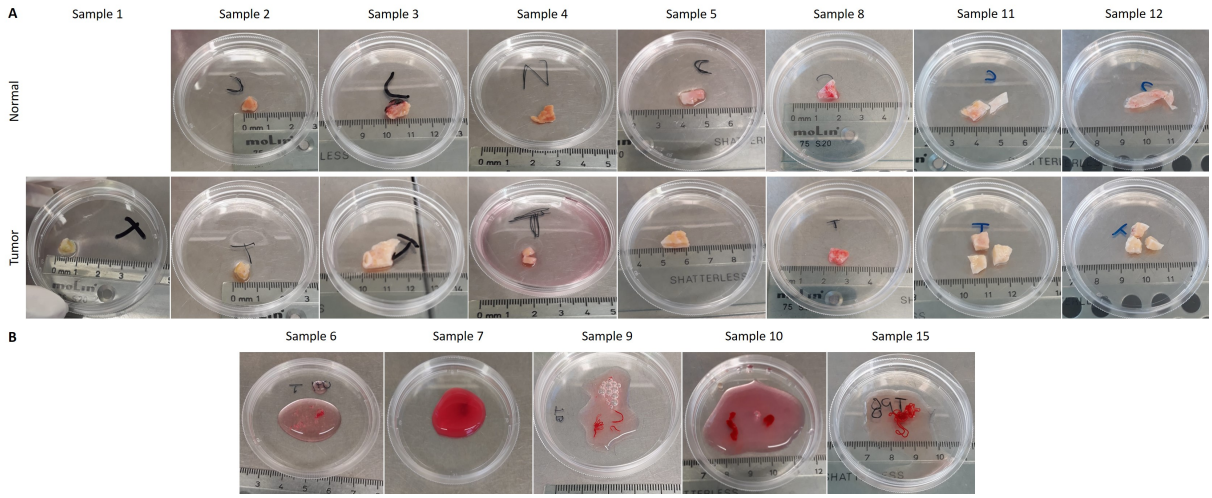

Figure 3.1: **Photographs of the samples obtained from patients.** Samples from thirteen different patients were obtained. For eight patients (A) there were surgery resections of normal tissue (top) and tumor tissue (bottom). The photograph taken from sample 1 Normal was lost due to a technical error. For five patients (B), there were fine-needle biopsies, and in these cases, there was no Normal tissue.

30 minutes at 37°C with agitation. The homogenate was then diluted 1:1 with ice-cold BM to inactivate the Collagenase and filtered through a 70μm cell strainer (Corning; Reference 352350). The cell suspension was then centrifuged at 300xg for 10 minutes at 4°C, the supernatant was discarded, and the pellet washed with 5mL of ACK Lysing Buffer (ThermoFisher; Reference A1049201) if red blood cells were present. After a final wash with 5mL of DPBS, the pellet was resuspended in an appropriate volume of DPBS. After initial isolation from the tumor tissue, cells were seeded in phenol red-free Matrigel® (Corning; Reference 356237), previously thawed on ice, at a concentration of approximately 10,000 or more cells (or cell groups) per 10μL droplet of Matrigel. Droplets of 45μL of Matrigel were placed on a pre-warmed (37°C) 6-well plate. The plate was left upside down on an incubator at 37°C for 20 minutes to allow Matrigel to solidify, then 2mL of organoid complete medium was added. Organoid complete medium is BM supplemented with 100ng/mL Noggin (Peprotech; Reference 120-10C), 500ng/mL R-Spondin1 (Peprotech; Reference 120-38), 1X B27 (ThermoFisher; Reference 17504-044), 1.25mM N-Acetyl-L-Cysteine (Sigma; Reference A9165), 10mM Nicotinamide (Sigma; Reference N0636-100G), 5μM A83 01 (Sigma; Reference SML0788), 100ng/mL FGF-10 (Peprotech; Reference 100-26), 100ng/mL EGF (Peprotech; Reference AF-100-15), 0.01μM Human Gastrin I (Sigma; Reference G9020) and 1μM Prostaglandin E2 (Tocris; Reference 2296/10). 10μM ROCK inhibitor Y-27632 (StemCell Technologies; Reference 72304) was added to the complete medium upon initial plating of cells, then removed when the medium was changed. The medium was changed every two/three days, and the organoids were kept in a humidified incubator at $37°C$ with 5% CO_2.

For the generation of normal tissue organoids of samples 1 to 8 (Figure 3.2), samples were also washed with ice-cold DPBS and cut into small fragments in pre-warmed digestion buffer [BM containing 0.5mg/mL DNase I (Sigma; Reference 10104159001), 2mg/mL Trypsin from bovine pancreas (Sigma; Reference T9935) and 0.5mg/mL Type II Collagenase (ThermoFisher; Reference 17101-015)] using a scalpel or scissor. This homogenate was incubated for 30 minutes with agitation, then filtered and spun similarly to tumor samples. The following steps were as described previously for the generation of tumor organoids. For the generation of normal tissue organoids of samples 11 and 12, a new method was implemented for the collection of normal pancreatic duct, instead of pancreatic tissue. In these cases the samples were also washed with ice-cold DPBS and cut into small fragments in pre-warmed digestion buffer, that was also altered [BM containing 0.5mg/mL DNase I and 0.5mg/mL Type II Collagenase] using a scalpel or scissor. The following steps were as described above.

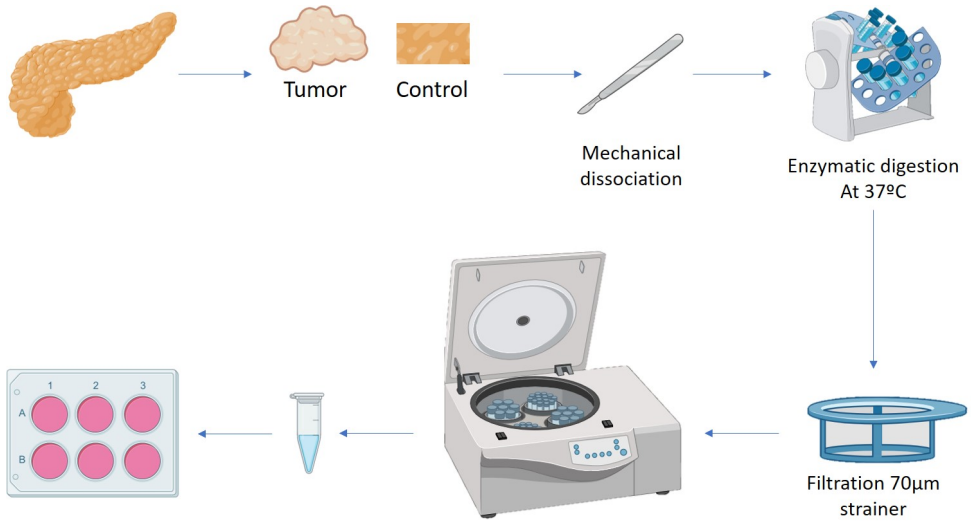

Figure 3.2: **Overview of the organoid culture protocol.** Tumor and normal samples are collected during surgery. For organoid generation, the tissue is mechanically and enzymatically dissociated (type II collagenase for tumors and a cocktail of type II collagenase and DNase I for normal tissue). Cell suspensions are filtered and centrifuged, and cells are resuspended in Matrigel and plated.

For the generation of tumor tissue organoids derived from FNB samples 6, 7 and 9, the protocol used was the same as in tumor samples. After Sample 10 (included) we optimized the protocol and the tissue was washed with 10mL of ice-cold DPBS and then 5mL of ACK Lysing Buffer. After the final wash with 5mL of ice-cold DPBS, the tissue was cut into small fragments in BM using a scalpel or scissor. These fragments were poured into pre-warmed (37$^{\circ}C$) BM containing Type II Collagenase (to obtain a final concentration of 2.5mg/mL) and incubated for 10/20 minutes at 37$^{\circ}C$ with agitation. The following steps were as described above.

Upon proper organoid maturation and growth under specified conditions, they were split at suitable ratios (typically between 1:1 to 1:3, depending on organoid confluency) every week.

For passaging (Figure 3.3), they were released from Matrigel using 1ml of pre-warmed (37°C) Accutase® solution (Sigma; Reference A6964), for up to 5 minutes at room temperature, then mechanically sheared through a P1000 pipette tip connected to a P200 or P10 pipette tip (without filter) and transferred to a Falcon® tube (Corning; Reference 430829) with 10mL of cold BM. This homogenate was centrifuged (10 minutes, 300xg, 4°C), the appropriate volume of the supernatant was removed, the cell pellet resuspended in Matrigel and seeded into pre-warmed 6-well culture plates. After 20 min upside-down on an incubator at 37°C, the Matrigel was overlaid with the respective complete medium. Organoid cultures were observed on a Zeiss Primovert bright-field inverted microscope, using 4x and 20x objectives, every day, and images were captured using a Zeiss AxioCam ERc5s camera.

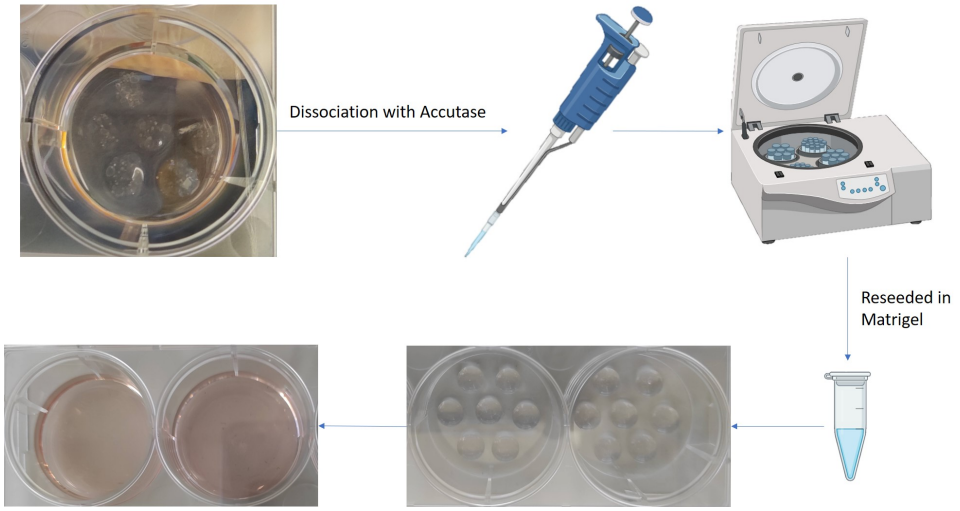

Figure 3.3: **Overview of the organoid passage protocol.** Once ready for passaging, organoids are dissociated from Matrigel with Accutase solution and mechanically sheared through a P1000 pipette tip connected to a P200 pipette tip without filter. Organoid fragments are collected by centrifugation, resuspended in the appropriate volume of medium and reseeded in Matrigel as for initial culture.

Organoid cultures should be closely monitored for the first few days after plating for potential bacterial and fungal infections [71]. If there is contamination in any culture plate and there are uncontaminated wells in that plate, the contaminated well needs to be treated. When contamination occurred, 5M NaOH (Sigma; Reference S581) was immediately added to the infected wells, left for 1 hour, and the contents then completely removed. The contaminated well was washed after removing the organoid material and disinfected with 70% (v/v) ethanol (VWR Chemicals; Reference 20821.330). The culture plate lid was replaced, which should minimize the chance of the infection spreading to other wells [71]. After removing the disinfected content from the well completely, the other wells' medium was changed, and the plate was placed for observation over the next few days. Once the culture is free of contamination for five days, the plate can be used for further culture [86].

Organoids were cryopreserved with 3dGRO™ Organoid Freeze Medium (Merck, Reference SCM301) according to manufacturers cryopreservation protocol. The culture medium was aspirated, and 1mL of 1x DPBS was added to each well. Using a p1000 pipette, the organoids were break up by pipetting up and down ten times and transferred to a 50mL Falcon tube. The mixture was centrifuged at 300xg for five minutes at 4°C, and the supernatant was removed. 10mL of BM was added to wash the pellet, and the suspension was centrifuged at 300xg for 10 minutes at 4°C. The supernatant was aspirated, leaving around 50-100μL of medium behind. The organoid pellet (over 200 organoids) was resuspended in 1mL of ice-cold 3dGRO™ Organoid Freeze Medium. 1mL was transferred into each labeled cryovial, placed in a Mr. Frosty™ container (ThermoFisher; Reference 5100-0001) filled with isopropyl alcohol. The freezing container was transferred to a -80°C freezer for 24 hours. For long-term storage, the cryovials were transferred to liquid nitrogen (-135°C).

3.3 Production of Wnt3a-conditioned medium

A cell line stably producing Wnt3a [L Wnt-3a cells (ATCC CRL® 2647™)] was used for the production of conditional medium, as briefly illustrated in Figure 3.4.

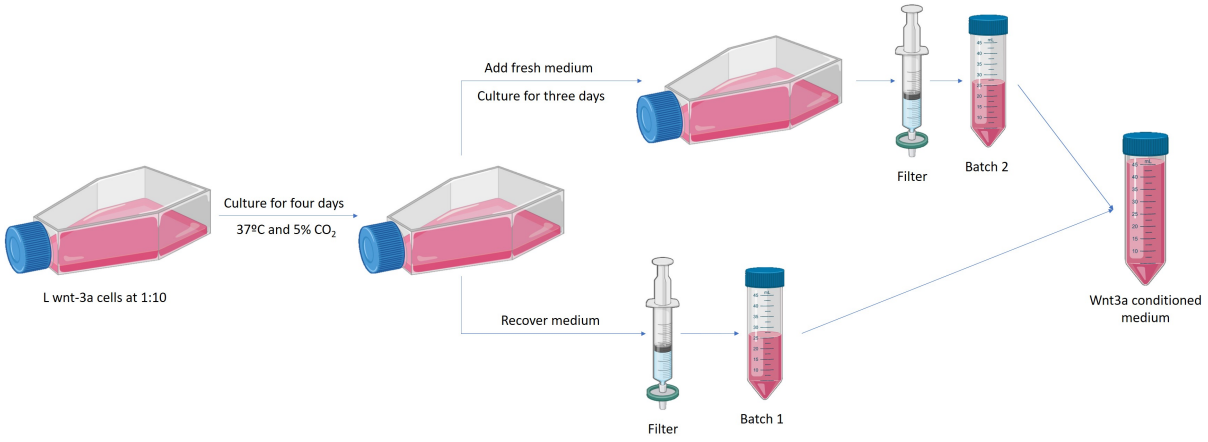

Figure 3.4: **Overview of the production of Wnt3a-conditioned medium.** Cells were thawed and seeded in complete growth medium. Cells were then split 1:10 in 10mL of culture medium without G-418. Upon culture for 4 days at 37°C and 5% CO_2, the supernatant was collected, filtered and stored at 4°C (first batch). The cells were cultured for another 3 days with 10ml of fresh medium for new collection of supernatant and filtration as before (second batch). To make the Wnt-3A conditioned medium the first and second batches were mixed 1:1.

Cells were defrost and seeded in complete growth medium [DMEM (ThermoFisher, Reference 41966-029), supplemented with 10% (v/v) FBS (ThermoFisher; Reference 10270-106) and 0.4mg/mL G-418 (Calbiochem; Reference 345810)]. Cells were then split 1:10 in 10mL of culture medium without G-418 in 75cm^2 flasks. Upon incubation for four days, the supernatant was collected, filtered through a 0.22μm filter with low protein binding (Merck; Reference

SLGVV255F), and stored at 4°C (first batch). The cells were incubated for three more days with 10ml of fresh medium for a new supernatant collection and filtered as before (second batch). Cells were discarded at this point due to being overgrown. The first and second batches were mixed 1:1 to make the Wnt-3A conditioned medium and store at 4°C or -20°C for long storage.

3.4 Histological analysis

When ready for organoid fixation, the medium was removed, and wells were washed twice with 1x PBS. 3mL of Formalin (Bio-Optica; Reference 05-01005Q) was added directly to the wells and incubated with mild fixed agitation for 1 hour. The organoids embedded in Matrigel were transferred to a 15mL Falcon® tube (Corning; Reference 352096) with a scrapper, and more formalin was added to a final volume of 8-10 mL. Fixed organoids were stored at room temperature, adequately identified, and protected from light until further processing. Histological analysis was done at the pathology department of Hospital da Luz Lisboa (Figure 3.5).

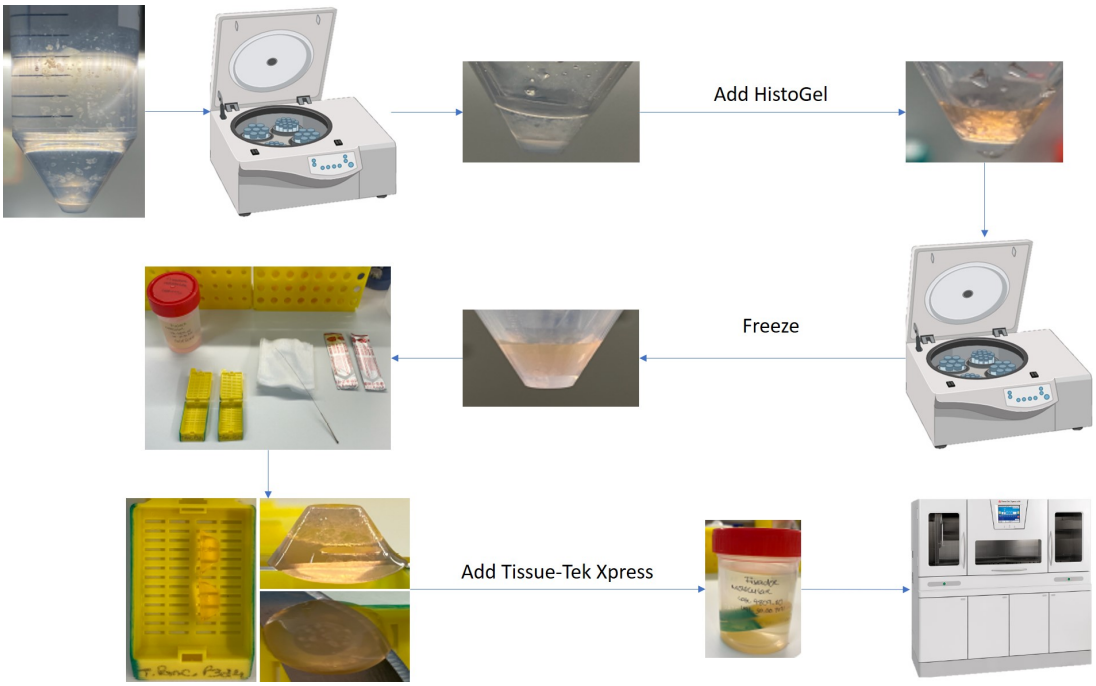

Figure 3.5: **Overview of the histology protocol.**The organoids were centrifuged and the supernatant was removed. The heated histogel was added to the pellet. This mixture was centrifuged and freezed at -20°C for five minutes. Using a scalpel, the gel was sliced and placed in a cassette. The cassette was placed in Tissue-Tek Xpress x120.

There, fixed organoids were centrifuged (five minutes, 1218xg), and the supernatant was removed. The centrifugation was repeated in order to extract as much as possible from the supernatant. The histogel (ThermoScientific; Reference HG-4000-012) was heated in a water bath in the microwave at 750W for one minute and 30 seconds, and six drops were added

to the pellet and mixed with the pipette. This mixture was centrifuged (one minute, 1912xg) and froze at -20$^{\circ}C$ for five minutes. With an acupuncture needle and the tube tilted down, air was created between the tube and the gel, causing it to come loose. The gel was sliced using a scalpel and placed in a cassette for processing histological material. The cassette was placed in Tissue-Tek Xpress® Molecular Fixative (Sakura; Reference 7120) for 15 minutes and then washed twice for 30 minutes in Tissue-Tek Xpress® Pre-Processing Solution (Sakura; Reference 7115). The cassette was then placed in Tissue-Tek Xpress® Molecular Fixative to be processed by Tissue-Tek Xpress® x120. Tumor organoids and primary patient tumor tissue were stained with Hematoxylin and Eosin (H&E) and compared by clinical pathologists.

3.5 Immunofluorescence microscopy

At the time points of interest, organoids were cultured in chamber slides. Upon organoid passaging, two Matrigel droplets of 10μL were plated in each well of a μ-Slide 8 Well chambered coverslip (ibidi, Reference 190130/1) and covered with 200μL of complete medium. Once ready for fixation, the medium was removed, the wells were rinsed with 1x PBS, and 300μL of 4% (w/v) PFA (Sigma; Reference P6148) in 1x PBS was added to each well, and the organoids were fixed for 20 minutes, at room temperature, with gentle swirling. Each well was washed with 300μL of 1x PBS, three times for 10 minutes each, and organoids were stored in 1x PBS at 4$^{\circ}C$ until proceeding for permeabilization. For permeabilization, PBS was removed, and 300μL of 0.5% (w/v) Triton™ X-100 (Sigma; Reference T9284) in 1x PBS was added to each well, for 20 minutes, at room temperature, with gentle swirling. Wells were then washed three times for 5 minutes each with 300μL of 1x PBS. Blocking was done by incubating the organoids with 150μL of 3% (w/v) BSA (Sigma; Reference A2153) in 1x PBS for 45 minutes at room temperature. Primary antibodies used were rabbit anti-Ki67 (abcam; Reference ab833) at 1/100 and mouse anti-EpCam conjugated with FITC (abcam; Reference ab8666) at 5μg/mL (2.5/100). Antibodies were diluted in 1.5% (w/v) BSA in 1x PBS, and the wells were incubated with 150μL of the respective antibodies in a dark, humid chamber, overnight at 4$^{\circ}C$. Each well was rinsed twice the next day, then washed three times for 10 minutes with 1x PBS containing 0.05% Tween® 20 (Sigma; Reference P1379). Secondary antibody used was goat anti-rabbit IgG DyLight® 594 (Vector Laboratories; Reference DI-1594) at 1/100, from a 1:1 stock in glycerol. This was also diluted in 1.5% (w/v) BSA in 1x PBS, and the wells were incubated with 150μL of the respective antibody, in the dark, for 1 hour at room temperature. Then, wells were rinsed twice and washed for 10 minutes with 300μL of 1x PBS containing 0.05% Tween® 20, followed by a 10-minute incubation with 300μL of 0.5μg/mL DAPI in PBS. The organoids were

then washed three times for 5 minutes each with 300μL of 1x PBS containing 0.05% Tween® 20. After the final wash, 100μL of mounting medium made in-house was added to each well, and the stained organoids were stored at 4$^{\circ}C$ in the dark until microscopic analysis. Mounting medium is 9.2mM p-Phenylenediamine (Sigma; Reference 695106) in 90% (w/v) sterile glycerol (Sigma; Reference G6279) and 1x PBS, pH 9.5. Images were acquired on a Zeiss LSM 710 confocal point-scanning microscope using the Plan-Apochromat 20x/0.8 M27 objective. Dylight® 594 was excited with the DPSS 561-10 laser, and DAPI fluorescence was detected using the Diode 405-30 laser. Each channel was recorded independently, and pseudocolor images were generated and superimposed.

3.6 Drug sensitivity and viability assay

To test patient-derived organoids' response to the chemotherapeutic drugs, organoids were dissociated and seeded in Matrigel into a 96-well plate. Upon organoid passaging, 10μL droplets were plated in each well of a black, clear flat-bottom 96-well plate (Tecan; Reference 30122306) and covered with 100μL of complete medium. After maturation of organoids (24 to 48 hours in culture), treatment with carboplatin (Sigma, Reference C2538; concentration range between 0 and 50μM), olaparib (Santa Cruz Biotechnology, Reference sc-302017; concentration range between 0 and 200μM) and SR-4835 (medchemexpress, Reference HY-130250; concentration range between 0 and 1μM) was started. The culture medium was changed to complete medium containing the different concentrations of drugs. At three to five days posttreatment, an equal volume (100μL) of CellTiter-Glo® 3D reagent (Promega, Reference G968B) was added to each well, and cell viability was determined by luminescent cell viability assay, as described below. Before adding either the medium containing the drugs or the CellTiter-Glo® 3D reagent, images were taken of all the wells used to allow visual control of the organoids.

To quantify the number of viable cells within one well, the CellTiter-Glo® 3D Viability Assay (Promega) was applied, according to the manufacturers' protocol [87]. The organoids were lysed with the CellTiter-Glo® 3D, and the luminescence was measured within 30 min after the start of the reaction using TECAN microplate reader (TECAN Infinite M200).

The drug concentrations used were as follows for Sample 1: Olaparib at 0μM (contained DMSO at a volume equal to the volume used in the highest Olaparib dose), 0.05μM, 0.5μM, 1μM, 10μM, 25μM, and 50μM; Carboplatin at 0μM (contained Milli-Q® H_2O at a volume equal to the volume used in the highest Carboplatin dose), 1μM, 2μM, 5μM, 10 μM, 25μM and 50μM, and SR-4835 at 0μM (contained DMSO at a volume equal to the volume used in the highest SR-4835 dose), 0.001μM, 0.01μM, 0.05μM, 0.1μM, 0.5μM, and 1μM.

From Sample 5 onward the concentrations of olaparib and SR-4835 were adjusted as follows: Olaparib at 0μM (contained DMSO at a volume equal to the volume used in the highest Olaparib dose), 6.25μM, 12.5μM, 25μM, 50μM, 100μM, and 200μM; and SR-4835 at 0μM (contained DMSO at a volume equal to the volume used in the highest SR-4835 dose), 0.0125μM, 0.025μM, 0.05μM, 0.1μM, 0.2μM, and 0.4μM.

Half-maximal inhibitory concentrations (IC_{50}) were calculated using GraphPad Prism 8 (Nonlinear regression, [Inhibitor] vs response (three parameters)).

Synergistic effects of combination treatment were assessed by calculating the combination index (CI) using the Chou Talay method [88]. CI was calculated dose-response curve parameters using the CompuSyn program [89], as a CI $<$ 1 indicates synergism, a CI = 1 indicates an additive effect, and a CI $>$ 1 indicates antagonism.

4 Results

We optimized an organoid derivation and culture protocol to generate organoids from pancreatic ductal adenocarcinoma (PDAC), successfully deriving organoids from tumor samples as well as normal tissue. The organoids generated were morphologically characterized and compared to the tissue of origin and used to test drug sensitivity. These assays' goal is to evaluate organoid use as a model for predicting the response of tumors to treatment. More specifically, to test new combinations of drugs, such as PARP inhibitor (PARPi) olaparib with the CDK12/CDK13 inhibitor (CDK12/CDK13i) SR-4835.

4.1 Patient-derived organoids are successfully generated

Human tumor tissue available for research is limited, as only a small number of PDAC patients are eligible for surgical intervention. We had access to eight surgery resection samples (normal and tumor tissue from each patient) and five FNB samples, as shown in Figure 3.1.

Tumor and normal tissue were obtained from consenting patients (Annex II) undergoing surgery and used for organoid derivation and histological analysis. Samples were collected from PDAC patients, but only seven successfully originated a stable organoid line. Maria Carmo-Fonseca's laboratory at Instituto de Medicina Molecular João Lobo Antunes had already successfully implemented a protocol for patient-derived ovarian cancer organoids generation and culture. Based on previous experience from the team in generating organoids, we decided

Table 4.1: *Identification of samples and patient-derived organoids.*

Sample No.	Surgery Date	Patient Ref.	No. of passages	Survival (Days)
1 Tumor	28/10/2020	-	10	56
1 Normal	28/10/2020	-	2	30
3 Tumor	10/11/2020	-	1	13
4 Tumor	07/01/2021	-	1	23
5 Tumor	12/01/2021	98T	24	149
8 Tumor	09/02/2021	75T	21	137 ongoing
10 Tumor	25/02/2021	76T	2	25
11 Tumor	16/03/2021	78T	16	104 ongoing
11 Normal	16/03/2021	78N	8	47
12 Tumor	18/03/2021	81T	18	102 ongoing
12 Normal	18/03/2021	81N	20	102 ongoing
15 Tumor	20/04/2021	89T	12	79 ongoing

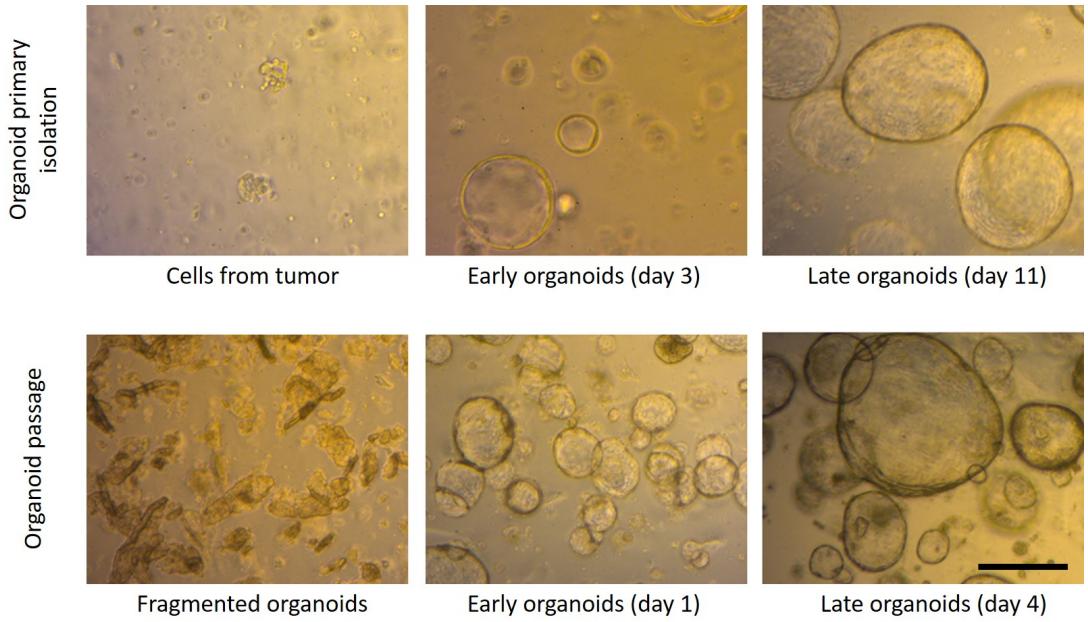

Figure 4.1: **Representative bright-field images of patient-derived organoids.** Primary organoid isolation (top) and first organoid passage (bottom) in different periods of maturation. The image represents the first organoid line successfully established in this work (Sample 1). There were no significant morphological differences identified allong the period in culture. Scale bar, 100μm.

to culture the cells in Matrigel, a substitute of extracellular matrix (ECM) commonly used for growing organoids [29]. For tissue dissociation and general culture medium conditions, we followed the work described by Hill et al. [3], Tsai et al. [77] and Tiriac et al. [23]. Using this method we managed to establish organoids from nine tumor samples (two being from FNB) and three normal samples (Table 4.1). Out of those, we were able to originate stable lines of organoids from six tumor samples (Figure 4.1) and one normal sample.

We were not able to generate stable lines of organoids from all samples. From Sample 2 and normal tissue from samples 4, 5, and 8, we could not dissociate the tissue and obtain viable cells. In tumor samples 3 and 4, organoids initially formed but could not be maintained after the first passage, as in normal tissue from Sample 1, that could not be maintained after the second passage, and normal tissue from Sample 11, that could not be maintained after the eight passage. In these samples, density became considerably lower, and there was a clear heterogeneity in organoid size, as well as signs of cell death. Following passage, organoids did not seem to recover, and the cultures were discontinued. Normal tissue from Sample 3 had contamination on the second day, so the culture was lost.

Sample 1 generated the first successfully established line of tumor organoids and was passed 10 times and expanded for 56 days. The second line (Sample 5) was passed 24 times and expanded for 149 days, the third line (Sample 8) was passed 21 times and expanded for 137 days, the fourth line (Sample 11) was passed 16 times and expanded for 104 days

and the fifth line (Sample 12) was passed 18 times and expanded for 102 days. Organoids were observed after just two days in culture in all samples. Following passage one, on day 12, organoids' growth rate from Sample 1 significantly increased, yielding higher densities. The same happened for Sample 5 and 8. Some passages had to be performed twice a week, instead of once a week (seven to ten days) as recommended by [90]. Following the third passage, the organoids of Sample 1 started showing signs of cell death (individual cells on the surface and around the organoids, and darkened structures) so they were concentrated rather than expanded on the fourth passage. After this passage, organoids recovered, growing in size and number. When observed on a bright-field microscope (Figure 4.1), organoid morphology seemed to be maintained through the period in the culture for all samples, without macroscopic changes in phenotype. The duration between passages varied, as each PDO culture has a growth rate based on poorly understood growth regulatory mechanisms [32]. The first passage of Sample 5 was after 14 days, as this culture harbors more dense organoids that grow slower. On the other hand, the first passage of Sample 8 was after just eight days because these organoids grew more rapidly. The proportion of small budding structures varied among donors, justifying these differences.

We were able to establish one stable line of normal tissue derived organoids (Sample 12 Normal), that was passed 20 times and expanded for 102 days - Table 4.1. Establishment efficiency was not very high for normal tissue, probably because the number of epithelial cells was low or the proliferation rate was slow. From Sample 11 forward the protocol of tissue collection changed and we were able to set up a protocol for normal pancreatic patient-derived organoid generation. The pathologist started to dissect the pancreatic duct tissue instead of pancreatic tissue. The digestion buffer was also changed, removing the trypsin, initially used.

Out of the five FNB samples received (Figure 3.1, B) only two were able to yield organoid isolates, Sample 10 and Sample 15. We were able to initially obtain organoids from Sample 10, but after the second passage organoid density became considerably lower and the culture could not be maintained. Sample 15 was passed 12 times and expanded for at least 79 days and characterization assays are ongoing. All the others samples failed because of the absence of viable epithelial cells from the specimens upon receipt in the laboratory, despite a visible core tissue sample on gross examination in the endoscopy procedure. Although at the optimizing phase the efficiency obtained with the protocol for FNB samples was low, after Sample 10 (when the protocol was optimized) we were able to establish a stable line of organoids. We improved the dissociation step of the protocol, that was first done for 30 minutes, and the digestion buffer used (see Chapter 3). We showed that it is possible to derive organoids from

FNB samples, but the efficiency is still low due to the limited sample size, making the number of epithelial cells low.

All stable organoid lines, except Sample 1 and 5 (that were frozen), continue expanding in culture after the writing of this thesis.

We were able to set up a protocol for patient-derived organoid generation and culture, having successfully derived and maintained stable lines of PDAC and normal pancreatic organoids. Our successful PDO culture derivation rate was: from tumor tissue 62.5% (5 from 8 attempts); from normal pancreatic duct 12.5% (1 from 8 attempts); and, most importantly, from FNB 20% (1 from 5 attempts).

4.2 Patient-derived organoids histologically recapitulate their tissue of origin

The definitive diagnosis of PC requires histopathological analysis. Hence, it is essential to characterize tumor-derived organoids before their use in downstream experimental procedures, including drug screening platforms [5]. Therefore, to evaluate whether our organoids resembled the parent tissue, a Hematoxylin and Eosin (H&E) staining was performed.

From a histologic point of view, the organoids showed clear similarities to their parent tumor. Morphological characterization of the PDAC organoids using standard H&E staining revealed globally spherical structures with cribriform architecture (Figure 4.2), a feature of complexity. Epithelium is predominantly multi-layered, with loss of nuclear polarity, and rare mitotic figures were observed. These characteristics are in line with the cytology expected for this type of tumor [70, 91, 92]. Additionally, typical nuclear features of malignancy were observed in all organoids, including nuclear enlargement, multiple nucleoli, and apoptosis. At different timepoints during culture, organoids were found in distinct stages of maturation, with differences in size and differentiation. PDAC is graded as well differentiated, moderately differentiated, or poorly differentiated [70] based on the assessment of gland formation, mitotic activity and nuclear features. Similar to the parental tumor, the organoids formed ducts with a cribriform growth pattern and cytonuclear atypia. Besides these glandular arrangements, fields of closely packed atypical cells with large abundant cytoplasm were observed. In well differentiated adenocarcinomas, such as sample 1 (Figure 4.2, A), it is possible to identify duct-like structures with angular contours and branching.

These results indicate that patient-derived tumor organoids retain most of the histological features of the tissue from which they were derived.

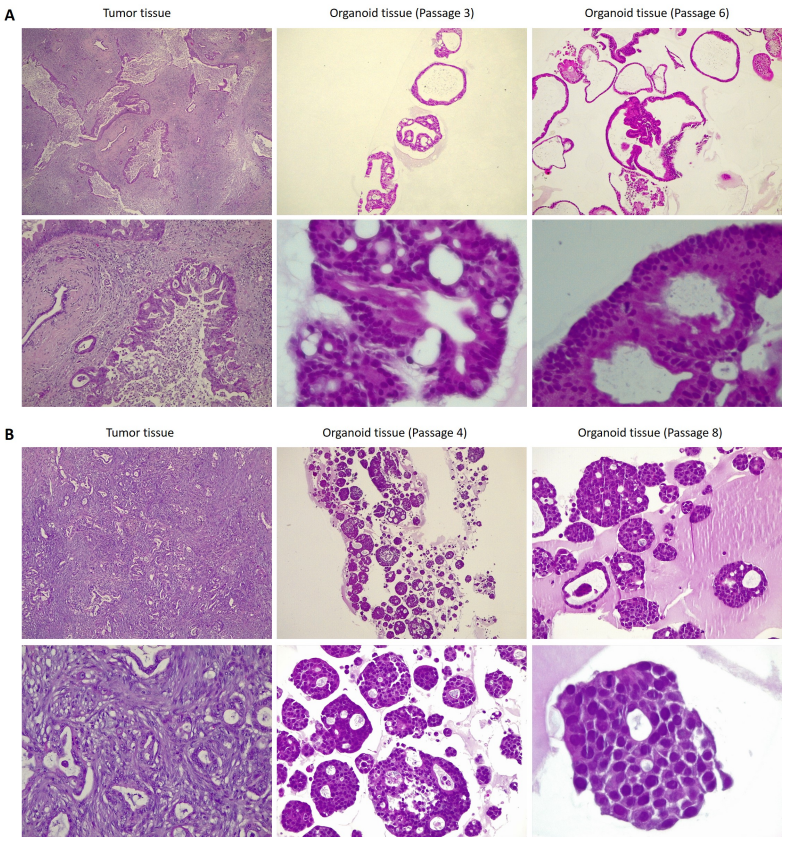

Figure 4.2: **Pancreatic ductal adenocarcinoma organoids histologically mimic the parent tumor from which they were derived.** Histological comparison of representative PDAC organoids (middle and right) to their corresponding tumor tissue (left) by H&E. (A) Organoids - at different time-points during culture (passage three and six) - and tumor derived from Sample 1. (B) Organoids - at different time-points during culture (passage four and eight) - and tumor derived from Sample 5.

4.3 Immunofluorescent staining allows determination of tumor organoid structural organization

Whole mount confocal immunofluorescence analysis was performed to better understand the structural organization of the patient-derived organoids, using an anti-EpCAM antibody, a marker of epithelial cell membranes and DAPI to stain DNA. It became clear that tumor organoids formed dense and complex structures harboring multiple lumens that resemble solid tumor masses (Figure 4.3, see also Appendix Figures A.1, A.2 and A.3). It is also possible to see two different morphologies in organoids derived from different patients. They can appear as either cystic (Figure 4.3, A) or dense structures (Figure 4.3, B). These two different morphologies can also be seen through a bright-field microscope. In Figure 4.1 we can see the cystic morphology of Sample 1. The different 3D-forming ability among the tested organoids is likely due to the different expression levels of adhesion molecules, or their interaction with ECM proteins, as proposed by Hou et al. [93].

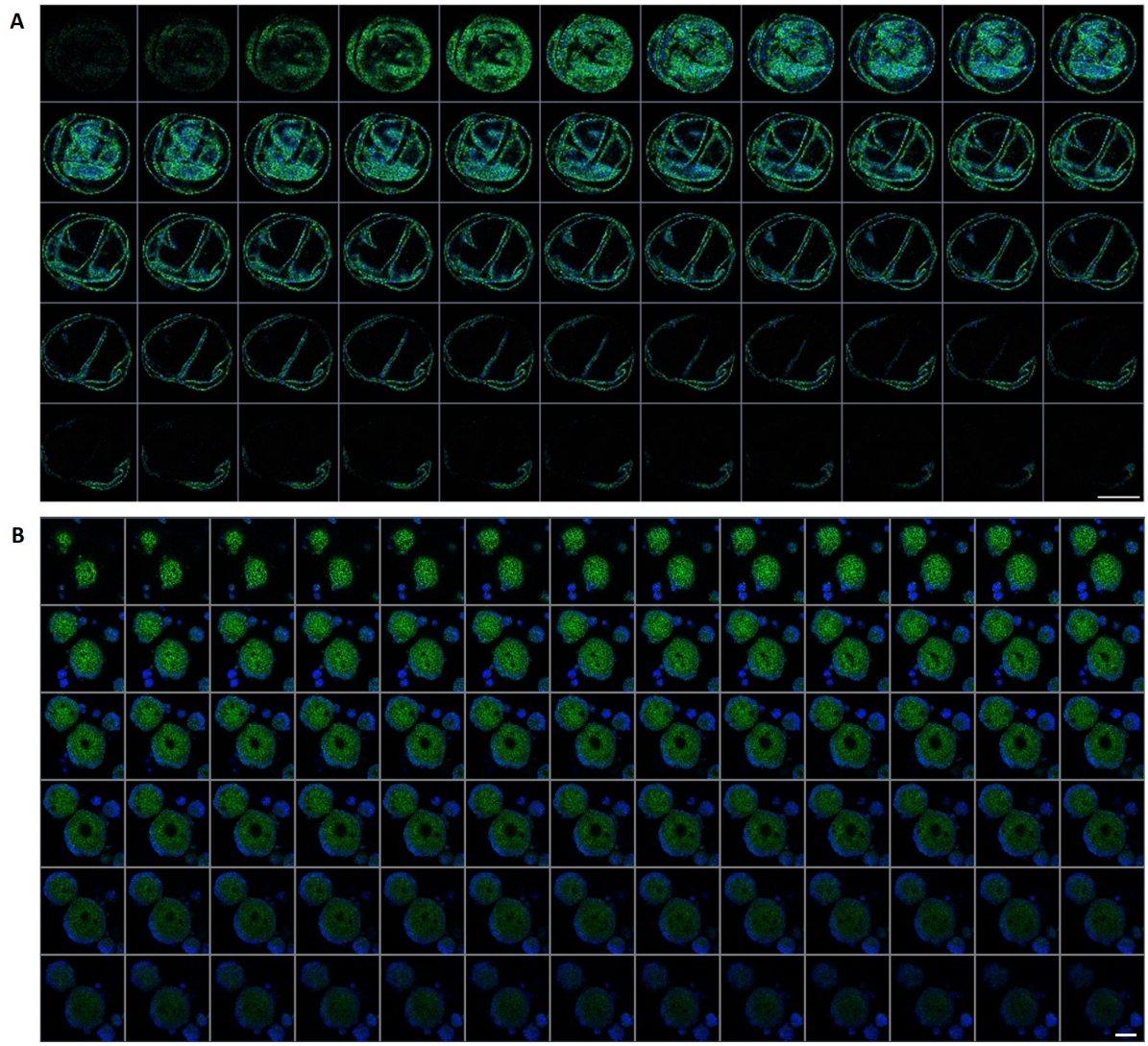

Figure 4.3: **Immunofluorescent staining of whole-mount patient-derived pancreatic ductal adenocarcinoma organoids.** Organoids were stained for the epithelial marker EpCAM (green) and nuclear marker DAPI (blue). (A) Organoids derived from Sample 1. Scale bar, 200μm. (B) Organoids derived from Sample 5. Scale bar, 100μm.

Whereas tumor organoids can appear as either cystic or dense structures, normal pancreatic ductal organoids appear as cystic structures (Appendix Figures A.4 and A.5) as previously described [90].

The observation that organoids displayed a fast growth rate in culture led us to use the Ki-67 nuclear marker to evaluate the proportion of proliferating cells in the organoids (Figure 4.4, see also Appendix Figure A.6). Indeed there was a high level of marked cells in all samples, which is concordant with the growth observed in culture.

With this analysis it is also possible to see that the organoids are heterogeneous in terms of size, as seen in Figure 4.4. Both images are from the same passage of Sample 1. The first organoid (top panel) is smaller and has bigger spaces between the nucleus. Moreover, the second one (bottom panel) is bigger, and the cells are more compacted.

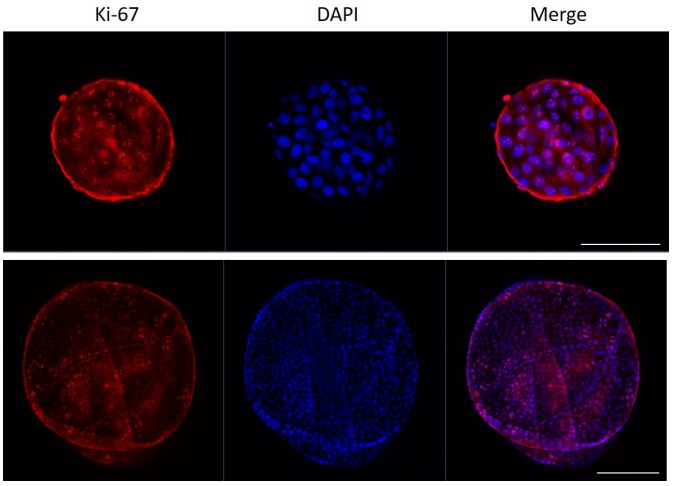

Figure 4.4: **Immunofluorescent staining of whole-mount patient-derived pancreatic ductal adenocarcinoma organoids using proliferation marker Ki-67.** Organoids were stained for the proliferation marker Ki-67 (red) and nuclear marker DAPI (blue). Tumor organoids display a high proportion of proliferating cells. It is possible to see a smaller organoid (top) compared with a bigger one (bottom). Organoids derived from Sample 1. Scale bar (top panel), 100μm, and (bottom panel), 200μm.

Collectively, these results demonstrate that our tumor organoids resemble a tumor mass's characteristics, not only in terms of cellular architecture but also in their ability to proliferate.

4.4 Tumor organoids lack therapeutic sensitivity to carboplatin, have different sensitivities to the PARPi Olparib and appear to be sensitive to the CDK12 inhibitor SR-4835

One of this project's goal was to determine if patient-derived pancreatic cancer organoids are a robust preclinical model for evaluating tumor response to therapy. Hence drug sensitivity assays were performed by measuring cell viability using the CellTiter-Glo® Luminescent Cell Viability Assay (Promega) (see Chapter 3). This method determines the number of viable cells in culture based on quantitation of the ATP present, an indicator of metabolically active cells. The luminescent signal generated after cell lysis is proportional to the amount of ATP present, which is directly proportional to the number of viable cells [87].

We started by testing organoids' response to the platinum-based drug carboplatin, the PARPi olaparib, and the CDK12/CDK13i SR-4835.

Despite the variability of the values, all the tumor organoids were resistant to carboplatin, with an IC_{50} superior to the concentrations tested (Figure 4.7, A, E, I, M, Q and U). The IC_{50} value indicates how much of a pharmacologic agent is required to inhibit a given biological activity by half [94]. The least resistant was Sample 15, that had the lower IC_{50} value (92.11μM). These results are similar to previous studies [23, 95], which revealed that organoids are resis-

tant to commonly used drugs that are non-targeted.

Regarding olaparib, the results had some differences in the different lines of tumor organoids, as can be seen in Figure 4.7 (B, F, J, N, R and V). Samples 5 and 15 were the only ones that seemed to be affected by olaparib (IC_{50} = 36.37μM and IC_{50} = 43.78μM, respectively). According to the IC_{50} values, cell viability of the other samples seems only to be affected at much higher concentrations of this drug. This may be related to the *BRCA* mutation status of the patients but this was not assessed in our study.

Tumor organoids displayed a high sensitivity to concentrations of SR-4835 above 0.2μM, and this agent appeared to be highly toxic to tumor tissue at the higher concentrations tested (Figure 4.7 C, G, K, O, S and W). Moreover, these results can be visually confirmed in Figure 4.5. In the bright-field images, it is possible to see the drugs' effects by organoid death - loss of structure and appearance of darkened structures.

For the first sample tested (Figure 4.7, A, B, C and D) we used concentrations previously described [23, 52, 83] and based on the initial results obtained we changed the concentrations of the drugs for the other samples taking into account the IC_{50} calculated. All the other samples were tested with the same concentration values.

We were also able to establish a line of normal tissue organoids (Sample 12 Normal) and we decided to evaluate these organoids' response to the same drugs used in the tumor organoids (Figure 4.6). We observed that this organoid line, unlike tumor organoids, displayed a high sensitivity to small doses of carboplatin (Figure 4.6, A), with an IC_{50} of 9.96μM, suggesting the toxicity of this drug to normal cells. This is expected taking into account the mechanism of action of this drug [96]. Despite being normal cells, in culture they are stimulated to proliferate and therefore it is expected that they will be affected by this cytotoxic activity. Alike PDAC organoids (Sample 12), no effect was observed with olaparib (Figure 4.6, B). This was expected taking into account the mechanism of action of this drug [14], because the normal cells are expected to be HR efficient and therefore insensitive to olaparib. Normal organoids exhibit a similar behavior, when comparing with tumor organoids, relative to the CDK12/CDK13i SR-4835, showing sensitivity to this agent (IC_{50} of 0.10μM). It was previously shown that the knockdown of CDK12 leads to significantly lower levels of *BRCA1*, resulting in genomic instability [57], therefore it is expected that inhibition of CDK12 will have an effect on normal cells, specifically if we take into account that the organoids are stimulated to proliferate.

Taken together, these results support the hypothesis that specific targeted therapies will be effective in only a subset of patients, and, as such, a personalized approach will be required to select the right drug for each individual patient, as showed before [21].

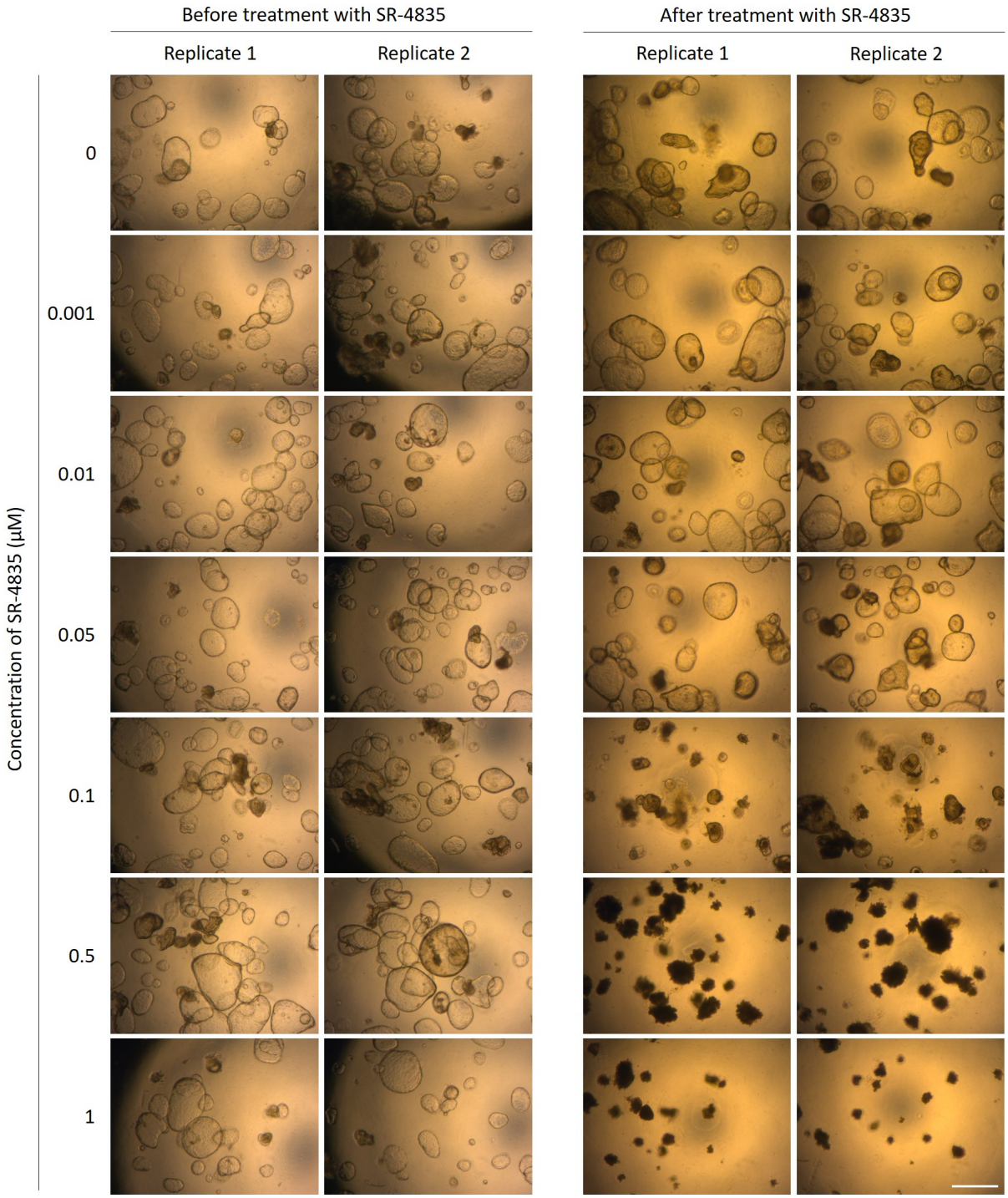

Figure 4.5: **Representative bright-field images of drug sensitivity assay with SR-4835.** Organoid droplets are imaged, using low magnification objectives to efficiently capture a wide field of view, using a bright-field microscope. Every droplet of Matrigel containing organoids, in the 96-well plate, is imaged before (left panel) and after (right panel) the drug treatment assay. Every assay has a technical duplicate. These images are from Sample 1. Scale bar, 200μm.

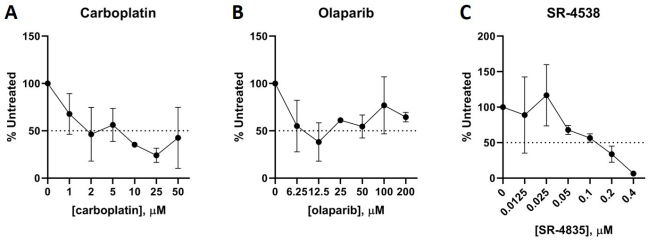

Figure 4.6: **Pancreatic ductal derived organoids seem sensitive to carboplatin and SR-4835.** Sensitivity dose curves of a normal pancreatic ductal organoid line (derived from Sample 12) to carboplatin (A), olaparib (B) and SR-4835 (C). Dots represent the mean of technical duplicates, and error bars represent the standard deviation of technical duplicates. A dashed line marks 50% untreated. IC_{50} for carboplatin = 9.96μM. IC_{50} for olaparib $>$ 1000μM. IC_{50} for SR-4835 = 0.10μM.

4.5 Tumor organoids have different sensitivities to the combination of PARPi Olparib and CDK12 inhibitor SR-4835

PDAC has been associated with significant levels of aberrations in CDK12 [55] and treatment with the CDK12/CDK13i SR-4835 potentiated BRCAness [1] phenotypes of triple-negative breast cancer cell lines and stimulated rapid tumor regression in multiple PDX mouse models [52]. Moreover, combining SR-4835 with olaparib or other DNA-damaging therapeutics was synergistic in triple-negative breast cancer cells [52]. Considering these results, we decided to investigate if CDK12 inhibition could be exploited in PDAC, namely to sensitize *BRCA* wild-type tumors to DNA-damaging drugs and to revert acquired resistance.

When testing two or more drugs in combination, it is essential not to overwhelm the cell with a lethal dose of a single agent as it will mask any synergistic effect of the combination [97]. The prerequisite for synergism or antagonism determination is to know both the "potency" and the "shape" of the dose-effect curve for each drug [88]. By first determining the IC_{50} for every single compound (see section 4.4), we can ensure that the combinations are performed at the proper dose ratio. We tested the organoids' response to a combination of SR-4835 with olaparib (Figure 4.7, D, H, L, P, T and X) to determine the effect of the combination. CDK12 inhibition seems to sensitize PDAC organoids to olaparib in all samples except Sample 5, given that the IC_{50} value of olaparib decreases with the combination of these drugs, relative to olaparib alone. In the case of Sample 5 (Figure 4.7, H) this value increases (from 36.37μM with olaparib to 50.90μM with the combination). Additionally, if we consider the first concentration point above the IC_{50} for each organoid (Table 4.2), we can see in the graphs (Figure 4.7) that the viability of organoids decrease with the combination of the drugs, compared to olaparib alone, for all

[1] BRCAness exists when an homologous recombination repair defect is present in a tumor in the absence of a germline *BRCA1* or *BRCA2* mutation. A BRCAness phenotype was thought to exist only in a small fraction of ovarian and breast cancers. However, more recently, it has become clear that significant proportions of pancreatic tumors, among others, might also exhibit BRCAness [51]

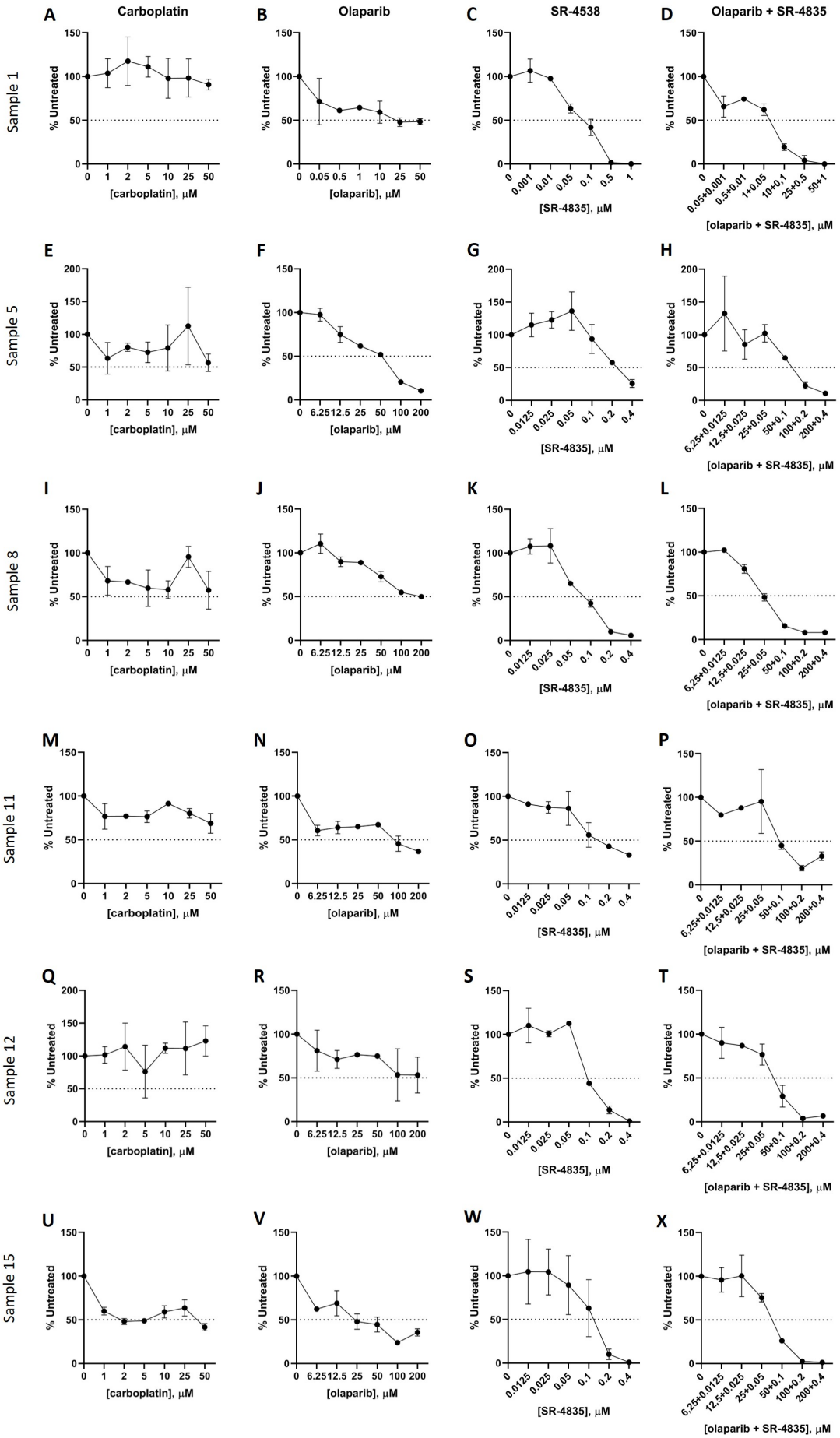
Carboplatin
Olaparib
SR-4538
Olaparib + SR-4835
Sample 1
Sample 5
Sample 8
Sample 11
Sample 12
Sample 15
A
B
C
D
E
F
G
H
I
J
K
L
M
N
O
P
Q
R
S
T
U
V
W
X
% Untreated
[carboplatin], μM
[olaparib], μM
[SR-4835], μM
[olaparib + SR-4835], μM

Figure 4.7: **Tumor organoids therapeutic sensitivity to olaparib, carboplatin and of SR-4835.** Sensitivity dose curves of pancreatic tumor organoid line of Sample 1 to carboplatin (A), olaparib (B), SR-4835 (C), and a combination of olaparib and SR-4835 (D). In (A) dots represent the mean of biological duplicates (passage 5 and 8), and error bars represent the standard deviation of biological duplicates. In (B), (C), and (D) assay was performed on passage 10, dots represent the mean of technical duplicates, and error bars represent the standard deviation of technical duplicates. IC_{50} for (A) = 266.40μM. IC_{50} for (B) = 63.07μM. IC_{50} for (C) = 0.06μM. IC_{50} for (D) = 2.57μM. Sensitivity dose curves of pancreatic tumor organoid line of Sample 5 to carboplatin (E), olaparib (F), SR-4835 (G), and a combination of olaparib and SR-4835 (H). IC_{50} for (E) = 382.90μM. IC_{50} for (F) = 36.37μM. IC_{50} for (G) = 0.23μM. IC_{50} for (H) = 50.90μM. Sensitivity dose curves of pancreatic tumor organoid line of Sample 8 to carboplatin (I), olaparib (J), SR-4835 (K), and a combination of olaparib and SR-4835 (L). IC_{50} for (I) = 379.60μM. IC_{50} for (J) = 137.70μM. IC_{50} for (K) = 0.07μM. IC_{50} for (L) = 20.33μM. Sensitivity dose curves of pancreatic tumor organoid line of Sample 11 to carboplatin (M), olaparib (N), SR-4835 (O), and a combination of olaparib and SR-4835 (P). IC_{50} for (M) = 245.50μM. IC_{50} for (N) = 148.80μM. IC_{50} for (O) = 0.17μM. IC_{50} for (P) = 58.28μM. Sensitivity dose curves of pancreatic tumor organoid line of Sample 12 to carboplatin (Q), olaparib (R), SR-4835 (S), and a combination of olaparib and SR-4835 (T). IC_{50} for (Q) $>$ 1000μM. IC_{50} for (R) = 230.30μM. IC_{50} for (S) = 0.09μM. IC_{50} for (T) = 29.22μM. Sensitivity dose curves of pancreatic tumor organoid line of Sample 15 to carboplatin (U), olaparib (V), SR-4835 (W), and a combination of olaparib and SR-4835 (X). IC_{50} for (U) = 92.11μM. IC_{50} for (V) = 43.78μM. IC_{50} for (W) = 0.09μM. IC_{50} for (X) = 28.49μM. In (E) to (X) the dots represent the mean of technical duplicates, and error bars represent the standard deviation of technical duplicates. A dashed line marks 50% untreated in all graphs.

samples, except Sample 5.

To determine the synergistic effect we calculated the Combination Index (CI) for each combined concentration used, using the software CompuSyn [89]. This is a widely used method for analyzing dose-effect relationships [98]. The CI is used to quantitatively depict synergism (CI $<$ 1), additive effect (CI = 1), and antagonism (CI $>$1) [99]. The assays for olaparib, SR-4835, and the combination were carried out on the same day, under standardized conditions and with technical duplicates. Only the average effect values for each drug concentration were used for the dose-effect data, as recommended by Chou [88].

This analysis indicated a synergism between olaparib and SR-4835 for all samples (CI $<$ 1, see Table 4.2) except for Sample 5, where the combination of the two drugs had an antagonistic effect in all points tested (with CI $>$1,04, see Table 4.2), suggesting that in patients that respond to olaparib, the combination is not beneficial.

Table 4.2: *Identification of synergism or antagonism in selected concentrations of drugs of patient-derived organoids.*

Sample	IC_{50} for olaparib (μM)	IC_{50} for combination (μM)	Concentration point selected (μM)	Combination Index value	Synergism or antagonism
1 Tumor	63.07	2.57	10	0.6	Synergism
5 Tumor	36.37	50.90	100	1.7	Antagonism
8 Tumor	137.70	20.33	50	0.9	Synergism
11 Tumor	148.80	58.28	100	0.3	Synergism
12 Tumor	230.30	29.22	50	0.5	Synergism
15 Tumor	43.78	28.49	50	0.8	Synergism

Overall, these results show a proof-of concept that CDK12/CDK13i sensitize PDAC organoids to PARPi. Our results are in line with previous studies [52]. Taken together our findings support the *in vitro* ability of our organoids to predict tumor responses to chemotherapy.

5 Discussion

Pancreatic ductal adenocarcinoma (PDAC) is a lethal and poorly understood malignancy with limited treatment options [100]. Although new targets and therapeutic approaches are often published, less than one-quarter of people with the most common cancers benefit from precision medicine today [101]. Besides the heterogeneity of the disease and the ongoing efforts to classify different subtypes of pancreatic cancer (PC) [33], only a few therapeutic options are used for most patients. Organoids are a recent technique that creates a bridge between the ease of conventional cell models and the applicability of the *in vivo* xenografts. They represent mini-avatars that can be 3D cultured *in vitro* from a wide range of cancers [78]. Human organoids' primary goal is their use in modeling human diseases to establish paradigms for drug screening, genotype-phenotype testing, and even biobanking for specific diseases and future personalized treatments, including cell therapies [102]. ASCO believes that cancer clinical trials are vital to inform medical decisions and improve cancer care and that all patients should have the opportunity to participate [45]. Patient-derived organoids (PDOs) can provide this link between research and patient participation. By providing access to the tumor cells, the patient is allowing research to personalized therapy.

This project aimed at investigating whether CDK12/CDK13 inhibition selectively sensitizes PDAC cells to PARP inhibitors (PARPi), generating patient-derived PDAC organoids to assess their use as a reliable preclinical model for predicting tumors' response to therapy. This chapter will discuss the results obtained and evaluate our findings, showing how it relates to the available literature. We will present some limitations and future work to overcome them.

5.1 Generation of patient-derived organoids

Monolayer cell cultures are adapted to grow on flat and rigid surfaces, inducing dramatic mechanical stresses not usually experienced by cells in the body. Therefore 3D environment of cancer cells affects their biology because of the different spatial organization of cell surface receptors engaged in cell-to-cell and cell-to-matrix interactions [103]. There are three methodologies to culture organoids, namely submerged culture (growth occurring within solid gels of

the extracellular matrix (ECM), submerged beneath tissue culture medium), air-liquid interface (grow organoids containing both epithelial cells and surrounding stroma, as a cohesive unit, directly from tissue fragments) and iPSCs or embryonic stem cells culture (entails directed differentiation to the target tissue of interest) [72]. We used the submerged culture method, the typically used method for pancreatic PDOs. A defining characteristic of submerged organoids is their possession of exclusively epithelial cells and absence of stroma [72]. We used ECM derived from Engelbreth–Holm–Swarm mouse sarcoma (in this case Matrigel, but could also be Basement Membrane Extract) that became the standard scaffold for 3D organoid culture [8], including pancreatic PDOs. Here we followed the procedure described by Hill et al. [3], Tsai et al. [77] and Tiriac et al. [23] for sample processing and culture medium conditions. Although establishment efficiency was not very high, we optimized a protocol for PDO generation and culture, having successfully derived pancreatic organoids.

In the work of Seppala et al. [32], one-third of cultures failed to transition from expansion phase to characterization, while in our work was one half. Their reasons for failure to expand were similar to ours. They included suspected microbial contamination (in our Normal sample 3) and unclear biomass loss likely due to disease biology and dependence upon growth factors in the medium. Organoid outgrowth efficiency is dependent on the quality of the sample obtained and the percentage of epithelial tumor cells in the sample, so it is essential to obtain tissue pieces from viable (tumor) tissue, which is often pink in color (Figure 3.1). In contrast, necrotic tissue may appear yellowish, and this necrotic (tumor) tissue has poor organoid-forming efficiency [71]. As we can see in Figure 3.1 our samples were small in size, reducing the possibility to obtain epithelial tumor cells, and the majority of the samples present a yellowish color, which may justify the outgrowth efficiency obtained here. Possible reasons for our specimens failing to generate an organoid culture include: a) the fact that the samples might be predominantly composed of stromal cells, b) the fact that there are not sufficient viable tumor cells to establish a culture and c) the fact that the sample is heterogeneous in what refers to the ratio of stem to differentiated cells [71], it may happen that our samples do not have stem cells.

In some cases (tumor tissue from Sample 3 and 4 and normal tissue from Sample 1 and 11), derivation's efficiency was low, and cultures could not be maintained after passage because the organoids did not grow back. Spatial proximity between organoids often promotes their growth [104], so it could be that the organoid density was low. Another possibility was that when split, the organoids were broken up too small, which has been reported as a factor leading to reduced efficiency of organoid formation [105] or to a high dilution rate [90].

Acquisition of chemo-naive patient samples is preferred for initial optimization of these methods [106], but this is not always possible. However, in our case, none of the patients received neoadjuvant chemotherapy. Nevertheless, the heterogeneous biology of pancreatic ductal adenocarcinoma (PDAC) impacts organoid establishment as some PDOs are fast-growing (example Sample 1) and others grow much slower (example Sample 5). Organoids derived from advanced cancers often grow slower than organoids derived from normal epithelium [5] due to a much higher rate of mitotic failure and subsequent cell death in tumor organoids.

Healthy human pancreas tissue has proven to be more challenging to recreate and expand in culture, as showed previously in Georgakopoulos et al. [79]. The efficiency of derivation was low, and most cultures could not be maintained after the first passage because the organoids did not grow back, so we were not able to establish an organoid line from all our samples of normal tissue. The pancreas is formed of two functionally distinct compartments [107]: the exocrine compartment (comprising duct and acinar cells) and the endocrine compartment (composed of the islets of Langerhans). Only pancreatic duct cells, but not endocrine or acinar cells, are able to form organoids, suggesting that pancreatic stem cells reside reside mainly in the ductal epithelium in a healthy pancreas and can contribute to tissue regeneration during injury and inflammation [84]. We showed that the method for collecting normal tissue is important, and we changed the dissection protocol, collecting only ductal tissue. We derived normal tissue organoids from Sample 11 onward when we started to dissect ducts to derive organoids. Seino et al. [19] often observed the outgrowth of normal pancreas organoids from PDAC specimens. Although we had no way to prove that this did not happen in our cultures, our organoids were shown to originate from epithelial cancer cells by immunostaining with EpCAM, a epithelial cell marker, used as a positive cancer marker in various cancer [95]. We could have used, for example, SMAD4, one signal transducer from TGF-β that mediates pancreatic cell proliferation and apoptosis and is specifically inactivated in half of advanced PC [108], to better distinguish our organoids.

The use of fine-needle biopsy (FNB) sampling for the creation of organoids at the time of initial cancer diagnosis has the potential advantage of providing personalized medicine options for all patients with this disease, not just the few who go for surgical resection [28, 109]. Additionally, FNB sampling–derived PDAC organoids allow for a more global and unbiased understanding of tumor biology in PC, allowing for tissue acquisition from the tumor before any neoadjuvant chemotherapy is provided. FNB sampling has a good potential for organoid creation because most patients will not undergo surgery, but all patients need a tissue diagnosis before initiating systemic therapies. Additionally, only a small amount of tissue is needed for

organoid establishment. In their work, Bian et al. [78], demonstrated, as a proof of concept, that the use of PDAC-derived organoids from FNB specimens is a promising strategy to obtain clean transformed material and can help to make better decisions for a particular patient. The outgrowth efficiency of organoids from biopsies, in the work of Driehuis [21], was 31%. We were able to yield organoid isolates from two FNB samples, Sample 10 and Sample 15, out of the five received in our work. It may be due to the low tumor cellularity present in the biopsied tissue. This might be especially relevant considering that pancreatic tumors generally contain non-epithelial (stromal) cells [90].

5.2 Medium conditions for growing patient-derived organoids

One of the critical aspects of developing organoids is defining the right cocktail of growth factors to supplement culture media, which differs based on the tissue of origin. Driehuis et al. [21] suggest that medium composition may have a selective impact on PDOs outgrowth. The work of Seino et al. [19] strongly suggests that the lack of WNT/R-Spondin selects for the most aggressive form of PDAC during the establishment steps and that the use of one medium or the other preselects specific subtypes of PDAC organoid. The selection pressure created by the addition or removal of growth factors also allows for enrichment of rare tumor-like cells [21]. Wnt proteins constitute a large family of secreted glycoproteins that control diverse aspects of embryonic development and adult homeostasis [110], so we decided to use a Wnt-conditioned medium in our work. Similar to the results of Huch et al. [111], our culture medium based on the Wnt activation allowed the unlimited expansion of duct fragments. Under these conditions, pancreatic duct cells upregulate the stem-cell marker Lgr5 (receptor for RSPO1) [111]. The quality of conditioned medium may also play a role in the proliferation of PDOs and may influence the results from batch to batch. The production and long-term conservation of recombinant, active stable WNT remain a technical challenge as showed previously [8]. However, in the present work, we did not see differences in cultures with the batch change.

Although Matsuura et al. [112] observed steady propagation with only EGF and Noggin, we decided to use a more complete medium. We tried to reduce the R-spondin in some of our samples (Sample 11 and 12), and the culture did not respond well, so we maintained the level of R-spondin in our medium. Our medium also contains TGF-β pathway inhibitors (A83-01 and Noggin), R-Spondin1, and Wnt3a-conditioned media, EGF, and Prostaglandin E2 that are required for organoid propagation [73].

Driehuis et al. [71] recommend adding additional antibiotics for samples taken from microbiome-positive areas, such as the colon or the oral mucosa, for the first two passages. Due to

the pancreas' proximal position with the colon, we could have added some antibiotics to our medium, according to this recommendation. However, we did not think it was necessary because our basic growth medium contains the standard cocktail of antibiotics. Hence we only had one contamination case out of all our samples.

5.3 Patient-derived organoids characterization

All patients in this study had a histologically confirmed diagnosis of PDAC. We performed Hematoxylin and Eosin (H&E) staining to evaluate whether our organoids resembled the parent tissue. In line with previous reports [70], our organoids showed clear similarities to their parent tumor, from a histologic point of view. H&E staining revealed globally spherical structures with cribriform architecture (Figure 4.2), a feature of complexity. Typical nuclear features of malignancy were observed in all organoids, including nuclear enlargement, multiple nucleoli, and apoptosis. Additionally organoids conserved inter-patient variation in tumor histoarchitecture, and maintain the differentiation status observed in the matched primary tumor.

We also used the whole-mount immunofluorescent staining method, which was shown to be the best for analysis centered on the detection of antibody signal in Broutier et al. [107]. Immunostaining revealed that all organoids were positive for Ki-67, indicative of a highly proliferative nature. This was compatible with the growth observed in culture. Organoids were shown to originate from epithelial cells by staining with antibodies to EpCAM, a positive epithelial cell marker [95], this ductal marker could show a purely ductal cell population [107].

Organoid models varied in shape and size, suggesting that they mimic the morphological heterogeneity of the primary tumors. The size and shape of our organoids can be seen either by the immunostaining assay and optical microscope. When observed under a bright-field microscope, we detected two distinct morphologies in our organoids, whereas tumor organoids can appear as either cystic (Samples 1, 12 and 15) or dense (Sample 5), normal organoids appear as cystic structures, as was previously described [90]. Some organoid cultures can show a mixed phenotype, showing both dense and cystic organoids [90]. Our samples 8 and 11 showed this mixed phenotype. However, this characteristic became progressively less significant, as the phenotype became homogeneous after several passages. Also, it was evident that tumor and normal organoid lines exhibited distinct spatial architectures, with normal organoids appearing as hollow structures with well-oriented epithelium and PDAC organoids forming denser and more complex structures with several lumens. Immunofluorescent analysis using Ki-67, a widely used marker of cell proliferation [113], revealed that organoids had a higher proportion of proliferating cells, concordant with the grow observed in culture.

Overall, our organoids revealed histology similar to the parent tissue, and their structural organization resembled that of human pancreatic ducts and solid tumors.

5.4 Drug treatment

By predicting patients' tumor responses to specific drugs using the organoids as "avatars", the individual patient's optimal treatment may be selected. Here we started by testing organoids' response to the platinum-based drug carboplatin. Carboplatin is, as oxaliplatin, an antineoplasic agent that interacts with DNA and form cross-links, resulting in an interruption in DNA synthesis leading to cytotoxic and antitumor effects [38, 96]. Despite the variability of the values, all the tumor organoids were resistant to carboplatin. Our results are in line with Tiriac study [23], which revealed resistance to all commonly used chemotherapeutics for PC, a common issue observed in several PDO cultures and encountered in the clinic.

Prior and ongoing preclinical and clinical research to develop targeted therapies for PDAC, including PARPi, as a single or combination agent has shown great promise [14]. Cancer cells with a mutation in *BRCA* treated with PARPi accumulate SSB, leading to DSB that are not repaired by the homologous recombination (HR) pathway, ultimately resulting in cell cycle arrest or death [41]. Using PARP inhibition to target a specific DNA-repair pathway has the necessary selectivity profile and a wide therapeutic window for *BRCA*-deficient cells [40]. In our work, we had some differences in the response to olaparib in the different lines of tumor organoids. Fong et al. [40] found that not all *BRCA1* or *BRCA2* carriers had a response to olaparib. According to this work, these differences in response could also have resulted from preexisting genetic resistance. However, we did not assess the genetic background of the patients or organoids. Sample 5 is sensitive to olaparib, which is concordant with Maenhoudt et al. [64] whose work revealed distinct sensitivities of the different organoid lines for the drugs, thereby indicating patients' tumor-dependent responses. At the same time, it exposed distinct efficiencies of the different drugs on individual tumor organoid lines.

Given these results in cancer therapy, an effective drug combination may be a better way to overcome this resistance. A combination of drugs may target multiple proteins or pathways aberrantly activated in disease (but not in normal cells), reducing the chances for a tumor to develop drug resistance by activating bypassing pathways compared to standard monotherapies [114]. Lord et al. [51] have shown that defects in CDK12 impair the transcription of key HR genes, including *BRCA1*, reducing the efficiency of HR itself and therefore causing PARPi sensitivity. The precise roles of CDK12 and CDK13 in transcription elongation and co-transcriptional mRNA processing are just beginning to be unraveled [115]. There is a need

for a continued effort to unravel the specific roles of CDK12 in cancer for it to be used as a biomarker for the purpose of patient stratification. Several clinical trials that include patients harboring CDK12 mutations as a cohort are underway [115]. Considering the results of a previous study on triple-negative breast cancer cell lines [52], we hypothesize that CDK12/CDK13 inhibitors (CDK12/CDK13i) would sensitize PDAC organoids to PARPi (in this case, olaparib). SR-4835, the CDK12/CDK13i used here, was shown to act in synergy with PARPi and DNA-damaging chemotherapeutics by suppressing the expression of the genes in the DDR pathway [115]. We have tested in our organoids the combination of a PARPi with a CDK12/CDK13i to determine if there is a synergistic effect between these two drugs. Drug combination experiments for systematic evaluation are a challenging task. There is still no standardized guideline to choose the optimal reference model to calculate the synergistic effect [114], so we used the Loewe additivity model, which defines the expected effect if a drug was combined with itself [114]. We used CompuSyn software [88], one of the most used standalone software packages to calculate the interaction score based on the Loewe model [114] and the combination index (CI). CDK12/CDK13 inhibition seems to sensitize PDAC organoids to olaparib in all samples except Sample 5, given that the olaparib IC_{50} decreases with the combination of these drugs and CI < 1. In Sample 5 the combination of the two drugs had an antagonistic effect in all points tested (with CI $>$1,04). Curiously this was the only sample that was sensitive to olaparib, suggesting that in patients that respond to olaparib, the combination is not beneficial.

According to Driehuis et al. [71], large organoids will introduce variability in the readout of the screen, so we decided to start the drug treatment on day one after the passaging of organoids. This allows for organoids to grow and be homogeneous in size.

We have also tried to develop organoids from normal ductal pancreatic tissue to use as a control in drug sensitivity assays because normal organoids can be generated and exploited for screening drugs that exclusively target tumor cells without harming healthy cells [116]. We have successfully generated one normal organoid line. Drug tests showed that, unlike tumor organoids, normal organoids displayed a high sensitivity to small doses of carboplatin. Alike PDAC organoids, no effect was observed with olaparib and they are sensitive to the CDK12/CDK13i SR-4835. However, normal organoid cultures may be rather heterogeneous in the ratio of stem cells to differentiated cells, and display a high expansion rate [71], because organoid growth media favor an undifferentiated and proliferative state of the cultures. Therefore, the response of these organoids to chemotherapeutics targeting proliferating cells (not targeted therapies that should affect only cells carrying tumor-specific genetic alterations) may not always indicate the response of healthy tissues *in vivo*.

Collectively, these results demonstrate the possibility of using patient-derived cancer organoids to assess sensitivity to anti-tumor drugs.

5.5 Limitations and future work

Some limitations of the organoid model should be acknowledged, including the higher costs of culture reagents and the labor-intensive aspects of maintaining organoid cultures than traditional cell culture. Organoid culture conditions do not enable the survival or outgrowth of non-epithelial cells [73] and also lack other cell types (such as blood vessels, stromal components, and immune cells) present in the tumor micro-environment, being an incomplete representation of the tumor [83]. However, recent developments show that tumor-associated fibroblasts or lymphocytes can be included in culture [70], providing an even better reflection of the original tumor. Co-culture with others cell types may allow better representation of tumor micro-environment in drug assays. The influence of different matrix components or CAFs on therapeutic response is worthy of future examination, as well as the inclusion of immune cells in the *ex vivo* culture systems [23, 25], to establish a platform for the study of immunotherapy in PC.

One major issue we faced, when performing the drug sensitivity assay, was the heterogeneity of organoid density between wells in the same plate, which might affected the results. Despite we did visual control, using microscopy trying to obtain a similar number of organoids in the replicates, the results showed some variance. So improvements need to be made in the drug sensitivity assays to reduce variability between replicates. This can be solved with high-throughput and automated organoid distribution, reducing variability. An example is one platform where organoids are templated from monodisperse Matrigel droplets encapsulated with a certain number of primary tissue cells [117]. This allows a cellular composition statistically consistent across individual Matrigel droplets, reducing manual manipulation induced variability [117]. Schuster et al. [83] created a platform that can automatically create dynamic chemotherapy regimens in many paralleled organoid cultures and can analyze organoid response in real-time, with deep learning techniques. This may be a future platform to optimize the use of PDOs in the clinic. Integrated multi-organoid model systems can detect these complex and multi-organ drug effects in a predictive and physiologically relevant manner, whereas single organoid systems cannot [118]. When performing the drug assays, we considered CI a cost-effective way to study the synergy of the two drugs, but our design may have several shortcomings. As an example, any outlier measurements will have a drastic influence on the synergy detection, and the pre-defined concentration points can easily miss a narrow synergistic dose window of new drug pairs [119]. This can be overcome in the future, doing triplicates

for all the experiments or using new drug concentrations based on our results. There is still a relatively poor understanding of the mechanisms that may lead to synergistic interactions between drugs in individual samples, and mechanism-unbiased approaches are therefore crucial for identifying new synergies.

Different research groups have performed drug screens on PDOs, with differences between protocols in drug exposure timing, organoid size, the timing of treatment start relative to the seeding of the organoids, and the ECM used [71]. Although technical variability can be minimized by adhering to good laboratory practices, absolute metrics (both biological and technical) will differ when different methodologies are applied [71]. We optimize a method to derive organoids from pancreatic tissue, dependent on the type of sample. The standardization of assays and culture conditions for patient-derived materials is an essential step in the organoid cultures. It is also essential to meet EMA and FDA standards if organoid-based screens are introduced into the clinic [71]. What is the appropriate size of organoids that are most representative of the tumor response to drugs? How long do organoids have to be exposed to drugs to mimic the drug-tumor response? These are important questions that can be addressed with an intensive study in organoids. By receiving more samples, we can experiment with different conditions to answer these questions.

For resections, it is important to obtain tumor fragments from different tumor areas to increase the chance that the resulting organoid culture represents the *in vivo* tumor heterogeneity. In our work, this was not possible because all tumor resections were from just one area of the tumor. A faithful recapitulation of tumor heterogeneity may require culture from multiple sites of a single tumor or different metastatic sites. Several examples of organoid cultures from multiple tumor regions indicate that these cultures can manifest distinct drug sensitivity profiles [72, 90]. For example, organoids from different metastases from a PDAC patient showed a similar response to three chemotherapy drugs, but different responses to a fourth, 5-FU [23]. We could change the collection method of our tumor tissue in the future, thus covering multiple tumor sites, improving the ability to recapitulate intratumor heterogeneity.

To bring PDO-based drug response assessment to the clinic, PDO establishment and drug screening need to be performed within a short time frame, preferably limited to the diagnosis-treatment interval. In line with previous studies [74], we demonstrated that PDO establishment and drug screening are feasible within three weeks. When translating results for the clinic, apart from considering *in vivo* tumor microenvironment, it is essential to consider other factors such as the general patient health, drug metabolism, patient pre-treatment, mode of action of the drugs tested, *in vitro* assay duration or culture artifacts [120, 121]. All this may influence patient

response or drug-screening results and should be considered when comparing organoid and patient response. In the future it will be essential to do a retrospective study with all our patients, where we could compare the results of our drug assays with patients' clinical outcomes.

Isolation of DNA and RNA from original patients' tissue should be done in the future as we obtain more and more significant samples because it is vital to characterize organoids' morphology and compare the DNA fingerprint of PDOs with the original tissue. We further hypothesize that cell death caused by the combination treatments results from the lethal accumulation of unrepaired DNA damage and defective DNA damage checkpoint mechanisms. Therefore, it will be important to assess DDR and checkpoint proficiency in treated cells. Results from COMPASS demonstrate that there are unique advanced PC genomic and transcriptomic subtypes with molecular heterogeneity between individual cases and with differing responses to chemotherapy [12, 122]. This was the first prospective evidence that molecular profiling that defines subtypes may predict differential responses to chemotherapy among patients with advanced PC with different RNA subtypes [12, 122]. All these different subtypes are now proposed to be associated with prognostic outcome and differential drug responsiveness according to different studies [8, 22]. Collisson et al. [22] showed on one hand that quasimesenchymal subtype lines were, on average, more sensitive to gemcitabine than the classical subtype. On the other, erlotinib was more effective in classical subtype cell lines. Their results further establish phenotypic differences between the classical and quasimesenchymal subtypes and suggested that drugs will show subtype specificity in PDAC. This shows the importance of combining agents with similar subtype specificity.

6 Conclusion

In this project, patient-derived organoids were successfully generated from pancreatic ductal adenocarcinoma and pancreatic ducts. All organoid lines were maintained for over seven weeks, during which we performed morphological characterizations of the organoids and evaluated their sensitivity to anti-cancer drugs.

Standard Hematoxilin and Eosin staining of organoids revealed similar histological features between them and the original tissue. Immunofluorescent staining highlighted structural differences either between different tumors as between tumor and normal organoids. Tumor organoids showed no sensitivity to carboplatin. As for the PARP inhibitor olaparib, the response is patient-dependent. The combination of olaparib with the CDK12/CDK13 inhibitor SR-4835 seemed synergistic in the majority of the cases. Normal organoids lacked therapeutic sensitivity to olaparib, but carboplatin seemed more lethal.

Organoid modeling is rapidly evolving, and although current challenges need to be addressed, we showed here that this approach would positively impact basic cancer research and clinical advance. The ultimate goal of these organoids would be to provide a preclinical platform for personalized medicine in oncological patients by correlating drug response to genomic, transcriptomic, and proteomic alterations. Patient-derived organoids profiling using next-generation sequencing of DNA and RNA combined with pharmacotyping may predict responses in patients with pancreatic cancer and provide a rationale for prioritizing therapeutic regimens.

Bibliography

[1] SNS. Cancro — portugal no top 10 europeu. URL https://www.sns.gov.pt/noticias/2018/01/31/cancro-taxa-de-sobrevivencia-no-mundo/.

[2] CUF. Cancro do pâncreas. URL https://www.cuf.pt/saude-a-z/cancro-do-pancreas.

[3] S. J. Hill, B. Decker, E. A. Roberts, N. S. Horowitz, M. G. Muto, M. J. Worley, C. M. Feltmate, M. R. Nucci, E. M. Swisher, H. Nguyen, et al. Prediction of DNA repair inhibitor response in short-term patient-derived ovarian cancer organoids. *Cancer discovery*, 8 (11):1404–1421, 2018.

[4] H.-D. Liu, B.-R. Xia, M.-Z. Jin, and G. Lou. Organoid of ovarian cancer: genomic analysis and drug screening. *Clinical and Translational Oncology*, pages 1–12, 2020.

[5] J. Drost and H. Clevers. Organoids in cancer research. *Nature Reviews Cancer*, 18(7): 407–418, 2018.

[6] A. Caldeira. Cancro do pancreas a crueza dos números e como inverter a tendência. *Saúde e bem-estar*, pages 16–19, 2020.

[7] U. E. Gastroenterology. Pancreatic cancer across europe. URL https://ueg.eu/files/771/b7ee6f5f9aa5cd17ca1aea43ce848496.pdf.

[8] P.-O. Frappart and T. G. Hofmann. Pancreatic ductal adenocarcinoma (PDAC) organoids: The shining light at the end of the tunnel for drug response prediction and personalized medicine. *Cancers*, 12(10):2750, 2020.

[9] A. M. Saad, T. Turk, M. J. Al-Husseini, and O. Abdel-Rahman. Trends in pancreatic adenocarcinoma incidence and mortality in the United States in the last four decades; a seer-based study. *BMC cancer*, 18(1):1–11, 2018.

[10] R. L. Siegel, K. D. Miller, and A. Jemal. Cancer statistics, 2020. *CA-A CANCER JOURNAL FOR CLINICIANS*, 70(1):7–30, 2020.

[11] S. R. Nelson, C. Zhang, S. Roche, F. O'Neill, N. Swan, Y. Luo, A. Larkin, J. Crown, and N. Walsh. Modelling of pancreatic cancer biology: transcriptomic signature for 3D PDX-derived organoids and primary cell line organoid development. *Scientific reports*, 10(1): 1–12, 2020.

[12] A. Lambert, L. Schwarz, I. Borbath, A. Henry, J.-L. Van Laethem, D. Malka, M. Ducreux, and T. Conroy. An update on treatment options for pancreatic adenocarcinoma. *Therapeutic advances in medical oncology*, 11:1758835919875568, 2019.

[13] A. Coetzee, R. Grose, and H. Kocher. Pancreatic cancer organotypic models. 2019.

[14] A. Bhalla and M. W. Saif. PARP-inhibitors in BRCA-associated pancreatic cancer. *JOP. Journal of the Pancreas*, 15(4):340–343, 2014.

[15] A. Kowalewski, Ł. Szylberg, M. Saganek, W. Napiontek, P. Antosik, and D. Grzanka. Emerging strategies in BRCA-positive pancreatic cancer. *Journal of cancer research and clinical oncology*, 144(8):1503–1507, 2018.

[16] B. Dictionary. Digestive system. URL `https://biologydictionary.net/digestive-system/`.

[17] L. Huang, A. Holtzinger, I. Jagan, M. BeGora, I. Lohse, N. Ngai, C. Nostro, R. Wang, L. B. Muthuswamy, H. C. Crawford, et al. Ductal pancreatic cancer modeling and drug screening using human pluripotent stem cell–and patient-derived tumor organoids. *Nature medicine*, 21(11):1364–1371, 2015.

[18] J. Iqbal, A. Ragone, J. Lubinski, H. Lynch, P. Moller, P. Ghadirian, W. Foulkes, S. Armel, A. Eisen, S. Neuhausen, et al. The incidence of pancreatic cancer in BRCA1 and BRCA2 mutation carriers. *British journal of cancer*, 107(12):2005–2009, 2012.

[19] T. Seino, S. Kawasaki, M. Shimokawa, H. Tamagawa, K. Toshimitsu, M. Fujii, Y. Ohta, M. Matano, K. Nanki, K. Kawasaki, et al. Human pancreatic tumor organoids reveal loss of stem cell niche factor dependence during disease progression. *Cell Stem Cell*, 22(3): 454–467, 2018.

[20] N. J. Roberts, A. L. Norris, G. M. Petersen, M. L. Bondy, R. Brand, S. Gallinger, R. C. Kurtz, S. H. Olson, A. K. Rustgi, A. G. Schwartz, et al. Whole genome sequencing defines the genetic heterogeneity of familial pancreatic cancer. *Cancer discovery*, 6(2): 166–175, 2016.

[21] E. Driehuis, A. van Hoeck, K. Moore, S. Kolders, H. E. Francies, M. C. Gulersonmez, E. C. Stigter, B. Burgering, V. Geurts, A. Gracanin, et al. Pancreatic cancer organoids recapitulate disease and allow personalized drug screening. *Proceedings of the National Academy of Sciences*, 116(52):26580–26590, 2019.

[22] E. A. Collisson, A. Sadanandam, P. Olson, W. J. Gibb, M. Truitt, S. Gu, J. Cooc, J. Weinkle, G. E. Kim, L. Jakkula, et al. Subtypes of pancreatic ductal adenocarcinoma and their differing responses to therapy. *Nature medicine*, 17(4):500–503, 2011.

[23] H. Tiriac, P. Belleau, D. D. Engle, D. Plenker, A. Deschênes, T. D. Somerville, F. E. Froeling, R. A. Burkhart, R. E. Denroche, G.-H. Jang, et al. Organoid profiling identifies common responders to chemotherapy in pancreatic cancer. *Cancer discovery*, 8(9): 1112–1129, 2018.

[24] Y. Matsushita, B. Smith, M. Delannoy, M. A. Trujillo, P. Chianchiano, R. McMillan, H. Kamiyama, H. Liang, E. D. Thompson, R. H. Hruban, et al. Biphenotypic differentiation of pancreatic cancer in 3-dimensional culture. *Pancreas*, 48(9):1225–1231, 2019.

[25] H. Tiriac, D. Plenker, L. A. Baker, and D. A. Tuveson. Organoid models for translational pancreatic cancer research. *Current opinion in genetics & development*, 54:7–11, 2019.

[26] P.-O. Frappart, K. Walter, J. Gout, A. K. Beutel, M. Morawe, F. Arnold, M. Breunig, T. F. Barth, R. Marienfeld, L. Schulte, et al. Pancreatic cancer-derived organoids – a disease modeling tool to predict drug response. *United European gastroenterology journal*, 2020.

[27] J. F. Lacomb, D. Plenker, H. Tiriac, J. C. Bucobo, L. S. D'souza, A. S. Khokhar, H. Patel, B. Channer, D. Joseph, M. Wu, et al. Single-pass vs 2-pass endoscopic ultrasound-guided fine-needle biopsy sample collection for creation of pancreatic adenocarcinoma organoids. *Clinical Gastroenterology and Hepatology*, 2020.

[28] H. Tiriac, J. C. Bucobo, D. Tzimas, S. Grewel, J. F. Lacomb, L. M. Rowehl, S. Nagula, M. Wu, J. Kim, A. Sasson, et al. Successful creation of pancreatic cancer organoids by means of EUS-guided fine-needle biopsy sampling for personalized cancer treatment. *Gastrointestinal endoscopy*, 87(6):1474–1480, 2018.

[29] L. A. Baker, H. Tiriac, H. Clevers, and D. A. Tuveson. Modeling pancreatic cancer with organoids. *Trends in cancer*, 2(4):176–190, 2016.

[30] V. P. Groot, N. Rezaee, W. Wu, J. L. Cameron, E. K. Fishman, R. H. Hruban, M. J. Weiss, L. Zheng, C. L. Wolfgang, and J. He. Patterns, timing, and predictors of recurrence

following pancreatectomy for pancreatic ductal adenocarcinoma. *Annals of surgery*, 267 (5):936–945, 2018.

[31] A. Oba, F. Ho, Q. R. Bao, M. H. Al-Musawi, R. D. Schulick, and M. D. Chiaro. Neoadjuvant treatment in pancreatic cancer. *Frontiers in oncology*, 10:245, 2020.

[32] T. T. Seppälä, J. W. Zimmerman, E. Sereni, D. Plenker, R. Suri, N. Rozich, A. Blair, D. L. Thomas, J. Teinor, A. Javed, et al. Patient-derived organoid pharmacotyping is a clinically tractable strategy for precision medicine in pancreatic cancer. *Annals of surgery*, 272(3): 427–435, 2020.

[33] R. Abbassi and R. M. Schmid. Evolving treatment paradigms for pancreatic cancer. *Visceral medicine*, 35(6):362–372, 2019.

[34] EMA. Conclusões científicas e fundamentos para a alteração dos resumos das características do medicamento, da rotulagem e do folheto informativo apresentados pela emea, . URL `https://www.ema.europa.eu/en/documents/referral/gemzar-article-30-referral-annex-i-ii-iii_pt.pdf`.

[35] EMA. Resumo das caracterÍsticas do medicamento, . URL `https://www.ema.europa.eu/en/documents/product-information/abraxane-epar-product-information_pt.pdf`.

[36] infarmed. Resumo das caracterÍsticas do medicamento, . URL `https://extranet.infarmed.pt/INFOMED-fo/detalhes-medicamento.xhtml`.

[37] infarmed. Resumo das caracterÍsticas do medicamento, . URL `https://extranet.infarmed.pt/INFOMED-fo/detalhes-medicamento.xhtml`.

[38] infarmed. Resumo das caracterÍsticas do medicamento, . URL `https://extranet.infarmed.pt/INFOMED-fo/detalhes-medicamento.xhtml`.

[39] K. L. Aung, S. Holter, A. Borgida, A. Connor, M. Pintilie, N. C. Dhani, D. W. Hedley, J. J. Knox, and S. Gallinger. Overall survival of patients with pancreatic adenocarcinoma and BRCA1 or BRCA2 germline mutation., 2016.

[40] P. C. Fong, D. S. Boss, T. A. Yap, A. Tutt, P. Wu, M. Mergui-Roelvink, P. Mortimer, H. Swaisland, A. Lau, M. J. O'Connor, et al. Inhibition of poly (ADP-ribose) polymerase in tumors from BRCA mutation carriers. *New England Journal of Medicine*, 361(2):123–134, 2009.

[41] A. Madariaga, S. Lheureux, and A. M. Oza. Tailoring ovarian cancer treatment: implications of BRCA1/2 mutations. *Cancers*, 11(3):416, 2019.

[42] F. Zheng, Y. Zhang, S. Chen, X. Weng, Y. Rao, and H. Fang. Mechanism and current progress of poly adp-ribose polymerase (PARP) inhibitors in the treatment of ovarian cancer. *Biomedicine & Pharmacotherapy*, 123:109661, 2020.

[43] M. B. Daly, R. Pilarski, M. B. Yurgelun, M. P. Berry, S. S. Buys, P. Dickson, S. M. Domchek, A. Elkhanany, S. Friedman, J. E. Garber, et al. Genetic/familial high-risk assessment: Breast, ovarian, and pancreatic, version 1.2020 featured updates to the NCCN guidelines. *JNCCN Journal of the National Comprehensive Cancer Network*, 18(4):380–391, 2020.

[44] S. Lheureux, C. Gourley, I. Vergote, and A. M. Oza. Epithelial ovarian cancer. *The Lancet*, 393(10177):1240–1253, 2019.

[45] P. A. Konstantinopoulos, B. Norquist, C. Lacchetti, D. Armstrong, R. N. Grisham, P. J. Goodfellow, E. C. Kohn, D. A. Levine, J. F. Liu, K. H. Lu, et al. Germline and somatic tumor testing in epithelial ovarian cancer: ASCO guideline. *Journal of Clinical Oncology*, 38(11):1222–1245, 2020.

[46] U. N. Vaishampayan. An evaluation of olaparib for the treatment of pancreatic cancer. *Expert Opinion on Pharmacotherapy*, pages 1–6, 2020.

[47] D. K. Armstrong, R. D. Alvarez, J. N. Bakkum-Gamez, L. Barroilhet, K. Behbakht, A. Berchuck, J. S. Berek, L. M. Chen, M. Cristea, M. DeRosa, et al. Ovarian cancer, version 1.2019 featured updates to the NCCN guidelines. *JNCCN Journal of the National Comprehensive Cancer Network*, 17(8):896–909, 2019.

[48] B. Kaufman, R. Shapira-Frommer, R. K. Schmutzler, M. W. Audeh, M. Friedlander, J. Balmaña, G. Mitchell, G. Fried, S. M. Stemmer, A. Hubert, et al. Olaparib monotherapy in patients with advanced cancer and a germline BRCA1/2 mutation. *Journal of clinical oncology*, 33(3):244, 2015.

[49] T. Golan, P. Hammel, M. Reni, E. Van Cutsem, T. Macarulla, M. J. Hall, J.-O. Park, D. Hochhauser, D. Arnold, D.-Y. Oh, et al. Maintenance olaparib for germline BRCA-mutated metastatic pancreatic cancer. *New England Journal of Medicine*, 381(4):317–327, 2019.

[50] K. Shindo, J. Yu, M. Suenaga, S. Fesharakizadeh, C. Cho, A. Macgregor-Das, A. Siddiqui, P. D. Witmer, K. Tamura, T. J. Song, et al. Deleterious germline mutations in patients with apparently sporadic pancreatic adenocarcinoma. *Journal of Clinical Oncology*, 35(30): 3382, 2017.

[51] C. J. Lord and A. Ashworth. BRCAness revisited. *Nature Reviews Cancer*, 16(2):110, 2016.

[52] V. Quereda, S. Bayle, F. Vena, S. M. Frydman, A. Monastyrskyi, W. R. Roush, and D. R. Duckett. Therapeutic targeting of CDK12/CDK13 in triple-negative breast cancer. *Cancer Cell*, 36(5):545–558, 2019.

[53] M. Krajewska, R. Dries, A. V. Grassetti, S. Dust, Y. Gao, H. Huang, B. Sharma, D. S. Day, N. Kwiatkowski, M. Pomaville, et al. CDK12 loss in cancer cells affects DNA damage response genes through premature cleavage and polyadenylation. *Nature communications*, 10(1):1–16, 2019.

[54] H. Paculová and J. Kohoutek. The emerging roles of CDK12 in tumorigenesis. *Cell division*, 12(1):1–10, 2017.

[55] G. Y. Lui, C. Grandori, and C. J. Kemp. CDK12: an emerging therapeutic target for cancer. *Journal of clinical pathology*, 71(11):957–962, 2018.

[56] F. Emadi, T. Teo, M. H. Rahaman, and S. Wang. CDK12: a potential therapeutic target in cancer. *Drug Discovery Today*, 2020.

[57] D. Blazek, J. Kohoutek, K. Bartholomeeusen, E. Johansen, P. Hulinkova, Z. Luo, P. Cimermancic, J. Ule, and B. M. Peterlin. The cyclin k/CDK12 complex maintains genomic stability via regulation of expression of DNA damage response genes. *Genes & development*, 25(20):2158–2172, 2011.

[58] A. P. Chirackal Manavalan, K. Pilarova, M. Kluge, K. Bartholomeeusen, M. Rajecky, J. Oppelt, P. Khirsariya, K. Paruch, L. Krejci, C. C. Friedel, et al. CDK12 controls G1/S progression by regulating RNAPII processivity at core DNA replication genes. *EMBO reports*, 20(9):e47592, 2019.

[59] E. Lim, S. F. Johnson, M. Geyer, V. Serra, and G. I. Shapiro. Sensitizing HR-proficient cancers to PARP inhibitors. *Molecular & cellular oncology*, 4(6), 2017.

[60] I. Bajrami, J. R. Frankum, A. Konde, R. E. Miller, F. L. Rehman, R. Brough, J. Campbell, D. Sims, R. Rafiq, S. Hooper, et al. Genome-wide profiling of genetic synthetic

lethality identifies CDK12 as a novel determinant of PARP1/2 inhibitor sensitivity. *Cancer research*, 74(1):287–297, 2014.

[61] S. F. Johnson, C. Cruz, A. K. Greifenberg, S. Dust, D. G. Stover, D. Chi, B. Primack, S. Cao, A. J. Bernhardy, R. Coulson, et al. CDK12 inhibition reverses de novo and acquired PARP inhibitor resistance in BRCA wild-type and mutated models of triple-negative breast cancer. *Cell reports*, 17(9):2367–2381, 2016.

[62] S. Liang, L. Hu, Z. Wu, Z. Chen, S. Liu, X. Xu, and A. Qian. CDK12: A potent target and biomarker for human cancer therapy. *Cells*, 9(6):1483, 2020.

[63] S. Dumont, Z. Jan, R. Heremans, T. Van Gorp, I. Vergote, and D. Timmerman. Organoids of epithelial ovarian cancer as an emerging preclinical in vitro tool: A review. *Journal of ovarian research*, 12(1):105, 2019.

[64] N. Maenhoudt, C. Defraye, M. Boretto, Z. Jan, R. Heremans, B. Boeckx, F. Hermans, I. Arijs, B. Cox, E. Van Nieuwenhuysen, et al. Developing organoids from ovarian cancer as experimental and preclinical models. *Stem cell reports*, 2020.

[65] Y. Maru, N. Tanaka, M. Itami, and Y. Hippo. Efficient use of patient-derived organoids as a preclinical model for gynecologic tumors. *Gynecologic Oncology*, 154(1):189–198, 2019.

[66] H. K. Kleinman and G. R. Martin. Matrigel: basement membrane matrix with biological activity. In *Seminars in cancer biology*, volume 15, pages 378–386. Elsevier, 2005.

[67] H. Clevers. Modeling development and disease with organoids. *Cell*, 165(7):1586–1597, 2016.

[68] D. Tuveson and H. Clevers. Cancer modeling meets human organoid technology. *Science*, 364(6444):952–955, 2019.

[69] O. Kopper, C. J. de Witte, K. Lõhmussaar, J. E. Valle-Inclan, N. Hami, L. Kester, A. V. Balgobind, J. Korving, N. Proost, H. Begthel, et al. An organoid platform for ovarian cancer captures intra-and interpatient heterogeneity. *Nature medicine*, 25(5):838–849, 2019.

[70] R. D. Vaes, D. P. van Dijk, T. T. Welbers, M. J. Blok, M. R. Aberle, L. Heij, S. F. Boj, S. W. Olde Damink, and S. S. Rensen. Generation and initial characterization of novel tumour organoid models to study human pancreatic cancer-induced cachexia. *Journal of cachexia, sarcopenia and muscle*, 2020.

[71] E. Driehuis, K. Kretzschmar, and H. Clevers. Establishment of patient-derived cancer organoids for drug-screening applications. *Nature Protocols*, 15(10):3380–3409, 2020.

[72] Y.-H. Lo, K. Karlsson, and C. J. Kuo. Applications of organoids for cancer biology and precision medicine. *Nature Cancer*, 1(8):761–773, 2020.

[73] S. F. Boj, C.-I. Hwang, L. A. Baker, I. I. C. Chio, D. D. Engle, V. Corbo, M. Jager, M. Ponz-Sarvise, H. Tiriac, M. S. Spector, et al. Organoid models of human and mouse ductal pancreatic cancer. *Cell*, 160(1-2):324–338, 2015.

[74] C. J. de Witte, J. E. Valle-Inclan, N. Hami, K. Lõhmussaar, O. Kopper, C. P. H. Vreuls, G. N. Jonges, P. van Diest, L. Nguyen, H. Clevers, et al. Patient-derived ovarian cancer organoids mimic clinical response and exhibit heterogeneous inter-and intrapatient drug responses. *Cell reports*, 31(11):107762, 2020.

[75] A. E. Vilgelm, K. Bergdorf, M. Wolf, V. Bharti, R. Shattuck-Brandt, A. Blevins, C. Jones, C. Phifer, M. Lee, C. Lowe, et al. Fine-needle aspiration-based patient-derived cancer organoids. *Iscience*, 23(8):101408, 2020.

[76] X. Li, L. Nadauld, A. Ootani, D. C. Corney, R. K. Pai, O. Gevaert, M. A. Cantrell, P. G. Rack, J. T. Neal, C. W. Chan, et al. Oncogenic transformation of diverse gastrointestinal tissues in primary organoid culture. *Nature medicine*, 20(7):769, 2014.

[77] S. Tsai, L. McOlash, K. Palen, B. Johnson, C. Duris, Q. Yang, M. B. Dwinell, B. Hunt, D. B. Evans, J. Gershan, et al. Development of primary human pancreatic cancer organoids, matched stromal and immune cells and 3D tumor microenvironment models. *BMC cancer*, 18(1):1–13, 2018.

[78] B. Bian, N. A. Juiz, O. Gayet, M. Bigonnet, N. Brandone, J. Roques, J. Cros, N. Wang, N. Dusetti, and J. Iovanna. Pancreatic cancer organoids for determining sensitivity to bromodomain and extra-terminal inhibitors (BETi). *Frontiers in oncology*, 9:475, 2019.

[79] N. Georgakopoulos, N. Prior, B. Angres, G. Mastrogiovanni, A. Cagan, D. Harrison, C. J. Hindley, R. Arnes-Benito, S.-S. Liau, A. Curd, et al. Long-term expansion, genomic stability and in vivo safety of adult human pancreas organoids. *BMC developmental biology*, 20(1):1–20, 2020.

[80] M. Takasato, X. E. Pei, H. S. Chiu, B. Maier, G. J. Baillie, C. Ferguson, R. G. Parton, E. J. Wolvetang, M. S. Roost, S. M. C. de Sousa Lopes, et al. Kidney organoids from human

iPS cells contain multiple lineages and model human nephrogenesis. *Nature*, 526(7574): 564–568, 2015.

[81] D. Gao, I. Vela, A. Sboner, P. J. Iaquinta, W. R. Karthaus, A. Gopalan, C. Dowling, J. N. Wanjala, E. A. Undvall, V. K. Arora, et al. Organoid cultures derived from patients with advanced prostate cancer. *Cell*, 159(1):176–187, 2014.

[82] G. Raimondi, A. Mato-Berciano, S. Pascual-Sabater, M. Rovira-Rigau, M. Cuatrecasas, C. Fondevila, S. Sánchez-Cabús, H. Begthel, S. F. Boj, H. Clevers, et al. Patient-derived pancreatic tumour organoids identify therapeutic responses to oncolytic adenoviruses. *EBioMedicine*, 56:102786, 2020.

[83] B. Schuster, M. Junkin, S. S. Kashaf, I. Romero-Calvo, K. Kirby, J. Matthews, C. R. Weber, A. Rzhetsky, K. P. White, and S. Tay. Automated microfluidic platform for dynamic and combinatorial drug screening of tumor organoids. *Nature communications*, 11(1):1–12, 2020.

[84] M. Hohwieler, M. Müller, P.-O. Frappart, and S. Heller. Pancreatic progenitors and organoids as a prerequisite to model pancreatic diseases and cancer. *Stem cells international*, 2019, 2019.

[85] Y. Saito. Establishment of an organoid bank of biliary tract and pancreatic cancers and its application for personalized therapy and future treatment. *Journal of gastroenterology and hepatology*, 34(11):1906–1910, 2019.

[86] M. Borowski, M. Giovino-Doherty, L. Ji, M.-J. Shi, K. P. Smith, and J. Laning. Basic pluripotent stem cell culture protocols. In *StemBook [Internet]*. 2012.

[87] P. Corporation. TECHNICAL MANUAL - CellTiter-Glo 3D Cell Viability Assay. 2015.

[88] T.-C. Chou. Theoretical basis, experimental design, and computerized simulation of synergism and antagonism in drug combination studies. *Pharmacological reviews*, 58(3): 621–681, 2006.

[89] T. Chou and N. Martin. Compusyn software for drug combinations and for general dose-effect analysis, and user's guide. *Paramus: ComboSyn Inc*, 2007.

[90] E. Driehuis, A. Gracanin, R. G. J. Vries, H. Clevers, and S. F. Boj. Establishment of pancreatic organoids from normal tissue and tumors. *STAR protocols*, 1(3):100192, 2020.

[91] J. Vazzano and W. Chen. Ductal adenocarcinoma, nos. URL https://www.pathologyoutlines.com/topic/pancreasductal.html.

[92] W. C. of Tumours Editorial Board. Digestive system tumours. In *WHO Classification of Tumours*, pages 322–332. IARC publications, 2019.

[93] S. Hou, H. Tiriac, B. P. Sridharan, L. Scampavia, F. Madoux, J. Seldin, G. R. Souza, D. Watson, D. Tuveson, and T. P. Spicer. Advanced development of primary pancreatic organoid tumor models for high-throughput phenotypic drug screening. *SLAS DISCOVERY: Advancing Life Sciences R&D*, 23(6):574–584, 2018.

[94] S. Aykul and E. Martinez-Hackert. Determination of half-maximal inhibitory concentration using biosensor-based protein interaction analysis. *Analytical biochemistry*, 508:97–103, 2016.

[95] S. I. Choi, A.-R. Jeon, M. K. Kim, Y.-S. Lee, J. E. Im, J.-W. Koh, S.-S. Han, S.-Y. Kong, K.-A. Yoon, Y.-H. Koh, et al. Development of patient-derived preclinical platform for metastatic pancreatic cancer: PDOX and a subsequent organoid model system using percutaneous biopsy samples. *Frontiers in oncology*, 9:875, 2019.

[96] A. N. do Medicamento e Produtos de Saúde. Resumo das caracterÍsticas do medicamento. URL https://extranet.infarmed.pt/INFOMED-fo/pesquisa-avancada.xhtml.

[97] R. A. Burkhart, L. A. Baker, and H. Tiriac. Testing susceptibility of patient-derived organoid cultures to therapies: pharmacotyping. In *Phenotypic Screening*, pages 253–261. Springer, 2018.

[98] T.-C. Chou and P. Talalay. Quantitative analysis of dose-effect relationships: the combined effects of multiple drugs or enzyme inhibitors. *Advances in enzyme regulation*, 22: 27–55, 1984.

[99] T.-C. Chou. Drug combination studies and their synergy quantification using the chou-talalay method. *Cancer research*, 70(2):440–446, 2010.

[100] H. C. Zhang and C. J. Kuo. Personalizing pancreatic cancer organoids with hPSCs. *Nature medicine*, 21(11):1249–1251, 2015.

[101] J. S. Boehm, M. J. Garnett, D. J. Adams, H. E. Francies, T. R. Golub, W. C. Hahn, F. Iorio, J. M. McFarland, L. Parts, and F. Vazquez. Cancer research needs a better map, 2021.

[102] M. A. Lancaster and M. Huch. Disease modelling in human organoids. *Disease models & mechanisms*, 12(7), 2019.

[103] S. D'Agosto, S. Andreani, A. Scarpa, and V. Corbo. Preclinical modelling of PDA: is organoid the new black? *International journal of molecular sciences*, 20(11):2766, 2019.

[104] H. Rogers, L. Letchford, S. Vieira, M. Garcia-Casado, M. Fekry-Troll, C. Beaver, R. Nelson, and M. Francies, Hayley nd Garnett. Passaging cancer organoid cultures. URL `https://www.protocols.io/view/passaging-cancer-organoid-cultures-bfe3jjgn`.

[105] A. Ruchinskas and J. Clinton. Protocol for the thawing, expansion, and cryopreservation of mouse small intestinal organoids, 2020.

[106] H. Tiriac, R. French, and A. M. Lowy. Isolation and characterization of patient-derived pancreatic ductal adenocarcinoma organoid models. *Journal of visualized experiments: JoVE*, (155), 2020.

[107] L. Broutier, A. Andersson-Rolf, C. J. Hindley, S. F. Boj, H. Clevers, B.-K. Koo, and M. Huch. Culture and establishment of self-renewing human and mouse adult liver and pancreas 3D organoids and their genetic manipulation. *Nature protocols*, 11(9):1724, 2016.

[108] X. Xia, W. Wu, C. Huang, G. Cen, T. Jiang, J. Cao, K. Huang, and Z. Qiu. SMAD4 and its role in pancreatic cancer. *Tumor Biology*, 36(1):111–119, 2015.

[109] F. Yang, H. Wang, X. Liu, N. Ge, J. Guo, S. Wang, X. Song, L. Cao, and S. Sun. EUS-guided fine-needle technique-derived cancer organoids: A tailored "shennong deity" for every patient with cancer. *Endoscopic ultrasound*, 8(2):73, 2019.

[110] E. Mihara, H. Hirai, H. Yamamoto, K. Tamura-Kawakami, M. Matano, A. Kikuchi, T. Sato, and J. Takagi. Active and water-soluble form of lipidated Wnt protein is maintained by a serum glycoprotein afamin/α-albumin. *Elife*, 5:e11621, 2016.

[111] M. Huch, P. Bonfanti, S. F. Boj, T. Sato, C. J. Loomans, M. Van De Wetering, M. Sojoodi, V. S. Li, J. Schuijers, A. Gracanin, et al. Unlimited in vitro expansion of adult bi-potent pancreas progenitors through the Lgr5/R-spondin axis. *The EMBO journal*, 32(20):2708–2721, 2013.

[112] T. Matsuura, Y. Maru, M. Izumiya, D. Hoshi, S. Kato, M. Ochiai, M. Hori, S. Yamamoto, K. Tatsuno, T. Imai, et al. Organoid-based ex vivo reconstitution of Kras-driven pancreatic ductal carcinogenesis. *Carcinogenesis*, 41(4):490–501, 2020.

[113] M. Jurikova, L. Danihel, Š. Polák, and I. Varga. Ki67, PCNA, and MCM proteins: Markers of proliferation in the diagnosis of breast cancer. *Acta histochemica*, 118(5):544–552, 2016.

[114] B. Yadav, K. Wennerberg, T. Aittokallio, and J. Tang. Searching for drug synergy in complex dose–response landscapes using an interaction potency model. *Computational and structural biotechnology journal*, 13:504–513, 2015.

[115] S. Tadesse, D. R. Duckett, and A. Monastyrskyi. The promise and current status of CDK12/13 inhibition for the treatment of cancer. *Future Medicinal Chemistry*, (0), 2020.

[116] H. Xu, X. Lyu, M. Yi, W. Zhao, Y. Song, and K. Wu. Organoid technology and applications in cancer research. *Journal of hematology & oncology*, 11(1):1–15, 2018.

[117] S. Jiang, H. Zhao, W. Zhang, J. Wang, Y. Liu, Y. Cao, H. Zheng, Z. Hu, S. Wang, Y. Zhu, et al. An automated organoid platform with inter-organoid homogeneity and inter-patient heterogeneity. *Cell Reports Medicine*, 1(9):100161, 2020.

[118] A. Skardal, T. Shupe, and A. Atala. Organoid-on-a-chip and body-on-a-chip systems for drug screening and disease modeling. *Drug discovery today*, 21(9):1399–1411, 2016.

[119] A. Ianevski, A. K. Giri, P. Gautam, A. Kononov, S. Potdar, J. Saarela, K. Wennerberg, and T. Aittokallio. Prediction of drug combination effects with a minimal set of experiments. *Nature machine intelligence*, 1(12):568–577, 2019.

[120] M. R. Junttila and F. J. De Sauvage. Influence of tumour micro-environment heterogeneity on therapeutic response. *Nature*, 501(7467):346–354, 2013.

[121] L. Moreira, B. Bakir, P. Chatterji, Z. Dantes, M. Reichert, and A. K. Rustgi. Pancreas 3D organoids: current and future aspects as a research platform for personalized medicine in pancreatic cancer. *Cellular and molecular gastroenterology and hepatology*, 5(3):289–298, 2018.

[122] K. L. Aung, S. E. Fischer, R. E. Denroche, G.-H. Jang, A. Dodd, S. Creighton, B. Southwood, S.-B. Liang, D. Chadwick, A. Zhang, et al. Genomics-driven precision medicine for advanced pancreatic cancer: early results from the compass trial. *Clinical Cancer Research*, 24(6):1344–1354, 2018.

Annex I Project approval

HOSPITAL BEATRIZ ÂNGELO

Exma. Senhora

Prof. Doutora Marília Lopes Cravo

Diretora do Serviço de Gastrenterologia do Hospital Beatriz Ângelo

Loures, 06 de novembro de 2020

***N/Ref.ª** 3391/2020_MJH/CMO/NO*

Estudo HBA n.º 517_LH n.º 224

Correio eletrónico e PMP

Assunto: *"CDK12: potencial alvo terapêutico no cancro do pâncreas?"*

Exma. Senhora Prof. Doutora Marília Cravo,

No seguimento da submissão a este Hospital do estudo melhor identificado em epígrafe, no qual V. Exa. participa na qualidade de Investigador Principal, temos o prazer de informar que a Comissão de Ética para a Saúde (CES) do HBA considera asseguradas as questões éticas relacionadas com a realização do estudo, pelo que deliberou a sua aprovação em reunião ordinária do dia 06 de novembro do corrente ano.

Com os nossos melhores cumprimentos, p/ Presidente

A Presidente da Comissão de Ética para a Saúde do HBA

Maria João Heitor

SGHL - Sociedade Gestora do Hospital de Loures, SA
Avenida Carlos Teixeira, 3 | 2674-514 Loures | Portugal
T +351 219 847 200 | F +351 219 847 209
geral@hbeatrizangelo.pt
Capital Social 3.313.000 Euros | Registo da C.R.C. de Lisboa e Contribuinte n.º 509 217 605
www.hbeatrizangelo.pt

Annex II Informed consent

HOSPITAL DA LUZ
LEARNING HEALTH
TRAINING, RESEARCH & INNOVATION CENTER

Consentimento Informado

Nome do Estudo: CDK12: potencial alvo terapêutico no cancro do pâncreas?
Investigador Principal: Marília Cravo
Morada do local onde decorre o estudo: Av. Carlos Teixeira 3, 2674-514 Loures
Contacto de Emergência: 919439192

INFORMAÇÃO AO DOENTE

Está a ser convidado/a a participar num estudo que está a decorrer no *Hospital Beatriz Ângelo.*

Antes de decidir se quer participar, é importante que compreenda o motivo da realização deste estudo, o modo como a sua informação será utilizada, o que é que o estudo envolve e os possíveis benefícios, riscos e desconfortos. Por favor leia atentamente esta informação e coloque todas as perguntas que entender. Poderá discutir este estudo com outras pessoas, como o seu médico de família e/ou a sua família, se o desejar. Tome o tempo que precisar.

A decisão de participar ou não neste estudo não afetará de modo nenhum o direito aos cuidados médicos que lhe são prestados, presentemente ou no futuro, nesta instituição.

QUAL É O OBJETIVO DESTE ESTUDO?
O objetivo deste estudo é tentar identificar um novo medicamento que aumente a eficácia da quimioterapia no tratamento do cancro do pâncreas.

PORQUE ESTOU A SER CONVIDADO/A A PARTICIPAR NESTE ESTUDO?
Porque lhe foi recentemente diagnosticado um cancro no pâncreas.

TENHO QUE PARTICIPAR NESTE ESTUDO?
Terá toda a liberdade para recusar-se a participar no estudo ou retirar o seu consentimento, suspendendo a participação em qualquer momento. A participação é voluntária e a sua recusa em participar não envolverá qualquer penalização ou perda de benefícios. A recusa ou abandono não colocarão, de modo algum, em risco o direito a receber tratamento ou assistência médica, presentemente ou no futuro, nesta instituição.

O QUE É QUE ENVOLVE A MINHA PARTICIPAÇÃO NESTE ESTUDO?
Pedimos-lhe autorização para utilizar parte da amostra tumoral colhida durante a cirurgia para realizar uma análise molecular, sem em nada prejudicar o seu manejo clínico. Todos os procedimentos feitos (nomeadamente a cirurgia) são necessários e seriam sempre feitos para o manejo da sua lesão.

QUAIS SÃO OS POSSÍVEIS RISCOS E BENEFÍCIOS DE PARTICIPAR NESTE ESTUDO?
Não existem riscos acrescidos ao participar neste estudo.

Benefícios
Ao participar neste estudo está-nos a ajudar a tentar encontrar uma melhor forma de tratar os doentes com cancro do pâncreas com quimioterapia, que poderá vir a beneficiar estes doentes no futuro.

QUAIS SÃO OS CUSTOS POR PARTICIPAR NESTE ESTUDO?

Não terá custos acrescidos por participar neste estudo, no entanto também não haverá qualquer remuneração por participar neste estudo.

COMO SERÁ MANTIDA A MINHA CONFIDENCIALIDADE NESTE ESTUDO?
Os registos são confidenciais e da responsabilidade dos investigadores. Os doentes serão identificados por número de série, ficando a identidade dos doentes envolvidos e os dados recolhidos apenas na posse da equipa de investigação. O nome dos doentes não será identificado em nenhum relatório ou publicação decorrente deste estudo. A informação recolhida será analisada como parte deste estudo. Esta informação poderá ser analisada por pessoas ou entidades autorizadas pelo investigador, de forma anonimizada, pela Comissão de Ética deste hospital, pelas Autoridades de Saúde, sob supervisão do seu médico, com o objetivo de confirmar a veracidade dos dados do estudo. Estes dados poderão ser comunicados a Autoridades Regulamentares. Os dados serão guardados durante o tempo exigido por lei.

A QUEM DEVO COLOCAR QUESTÕES SOBRE O ESTUDO?
O Médico Investigador poderá esclarecer qualquer dúvida que tenha. Os contactos são:

E-mail: __marilia.cravo@hbeatrizangelo.pt_____

Telefone:___919439192_____

CONSENTIMENTO INFORMADO

Ao assinar este Documento, declaro que:

- Li a informação descrita neste documento e foi-me dado tempo para refletir na minha participação no estudo;
- Tive oportunidade de colocar questões e obtive as respetivas respostas;
- Recebi uma cópia assinada e datada deste Consentimento Informado.

Nome Completo do Participante: _____

Data: …… Assinatura:……

Caso o Participante seja menor ou declarado interdito ou inabilitado nos termos legais, o consentimento do Participante pode ser expresso pelo seu representante legal:

Nome completo do Representante Legal: _____

Nº documento identificação:

Natureza da Representação Legal (selecionar o que for aplicável):

- ☐ Poder paternal (participante menor)
- ☐ Tutor (participante menor ou interdito)
- ☐ Curador (participante inabilitado)

Data..... Assinatura.....

HOSPITAL DA LUZ
LEARNING HEALTH
TRAINING, RESEARCH & INNOVATION CENTER

Nome Completo do Médico Investigador: _____

Data: ..... Assinatura: .....

Glsmed Learning Health, SA
Rua Carlos Alberto da Mota Pinto, 17 - 9º • 1070-313 Lisboa • Portugal
T. +351 351 213 138 260 • F. +351 213 530 292 • E. learninghealth@luzsaude.pt
Capital Social: 50.000€ • Registo da C.R.C. de Lisboa e Contribuinte nº 513 620 04

LUZ SAÚDE

Appendix A Immunofluorescent staining of organoids

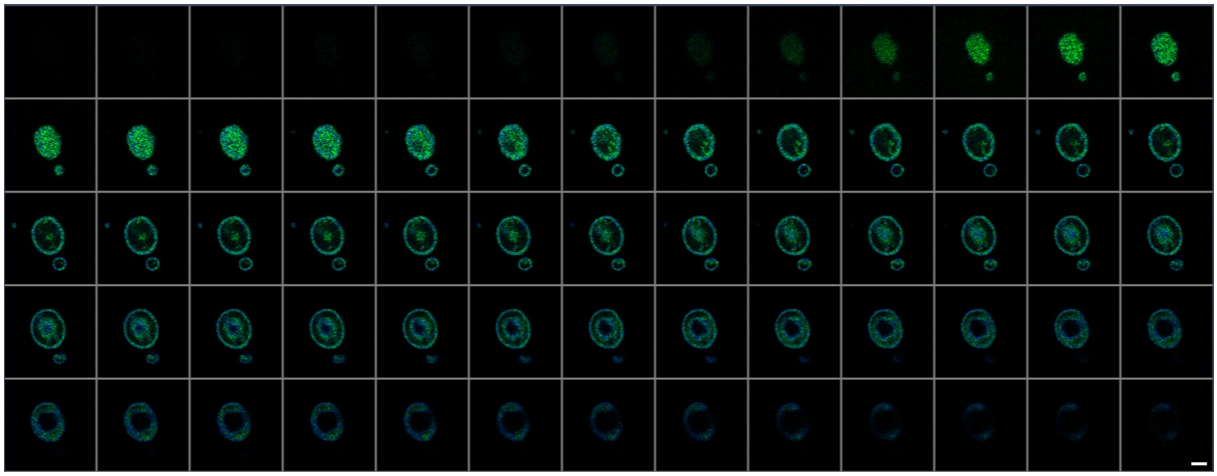

Figure A.1: **Immunofluorescent staining of EpCAM in whole-mount PDAC organoids derived from Sample 8.** Organoids were stained for the epithelial marker EpCAM (green) and nuclear marker DAPI (blue). Organoids derived from Sample 8. Scale bar, 100μm.

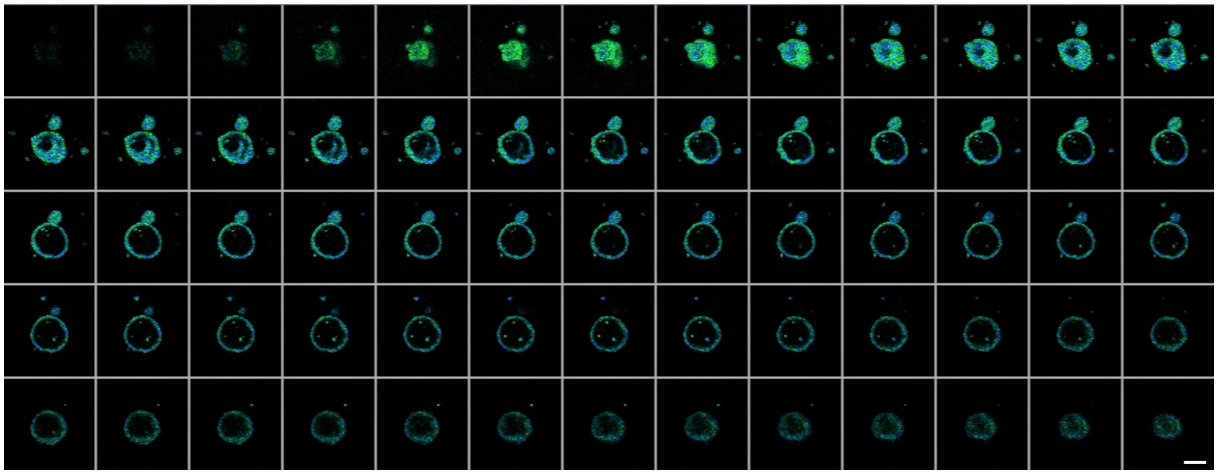

Figure A.2: **Immunofluorescent staining of EpCAM in whole-mount PDAC organoids derived from Sample 11.** Organoids were stained for the epithelial marker EpCAM (green) and nuclear marker DAPI (blue). Organoids derived from Tumor Sample 11. Scale bar, 100μm.

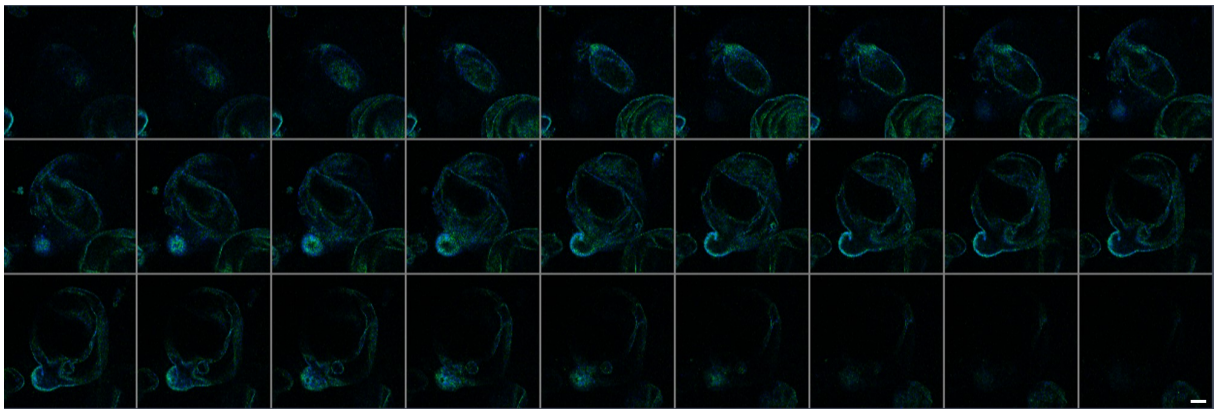

Figure A.3: **Immunofluorescent staining of EpCAM in whole-mount PDAC organoids derived from Sample 12.** Organoids were stained for the epithelial marker EpCAM (green) and nuclear marker DAPI (blue). Organoids derived from Sample 12. Scale bar, 100μm.

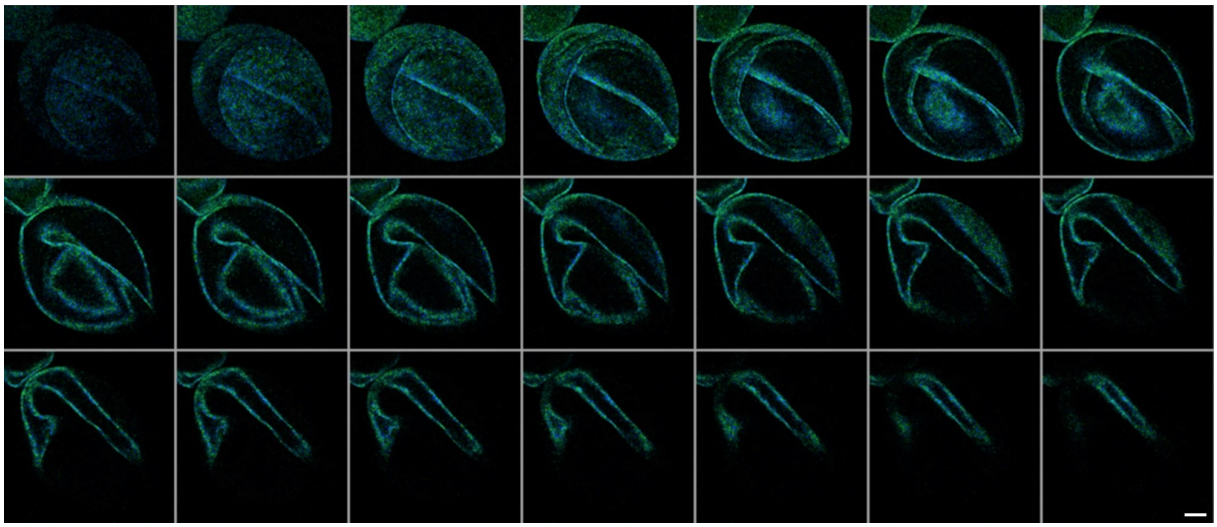

Figure A.4: **Immunofluorescent staining of EpCAM in whole-mount pancreatic duct organoids derived from Sample 11.** Organoids were stained for the epithelial marker EpCAM (green) and nuclear marker DAPI (blue). Organoids derived from Normal Sample 11. Scale bar, 100μm.

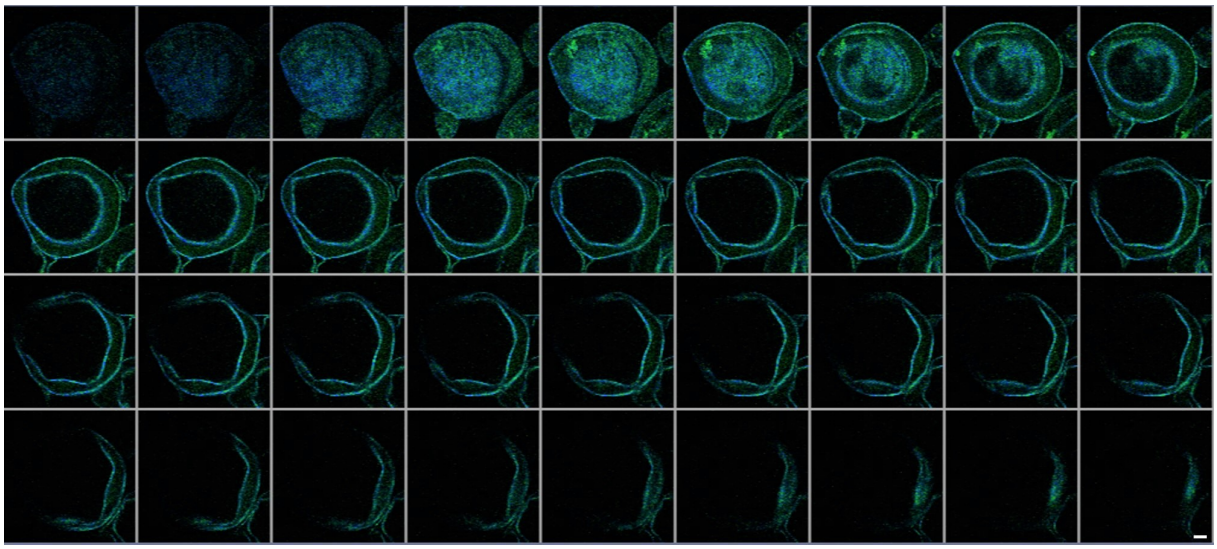

Figure A.5: **Immunofluorescent staining of EpCAM in whole-mount pancreatic duct organoids derived from Sample 12.** Organoids were stained for the epithelial marker EpCAM (green) and nuclear marker DAPI (blue). Organoids derived from Normal Sample 12. Scale bar, 100μm.

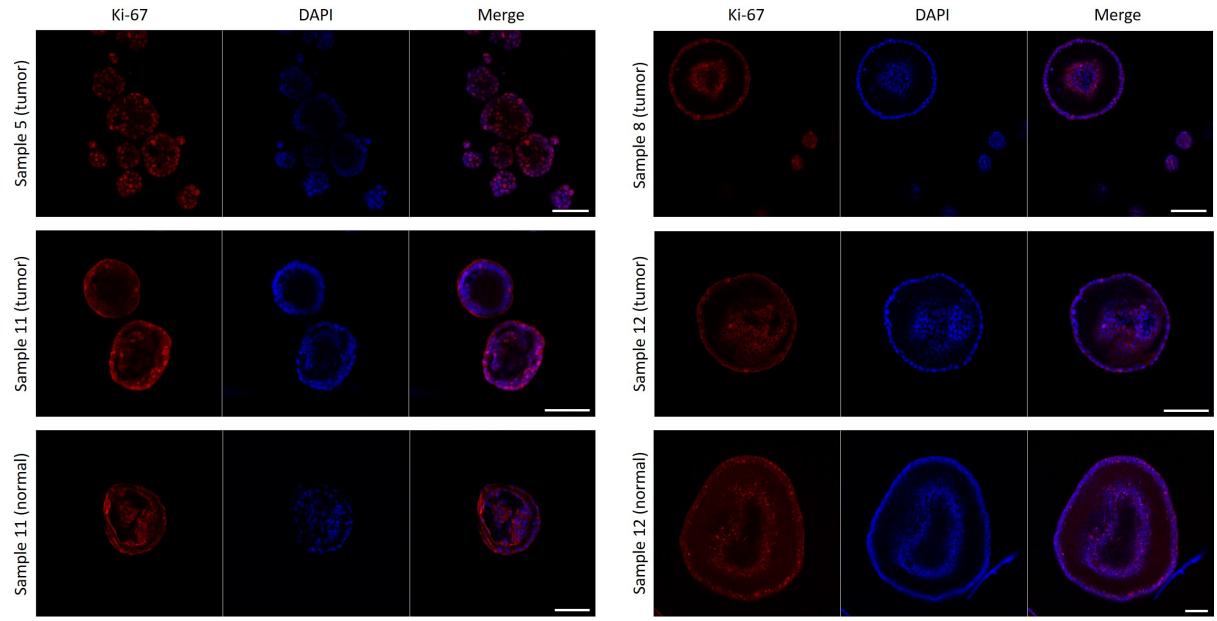

Figure A.6: **Immunofluorescent staining of whole-mount patient-derived pancreatic organoids using proliferation marker Ki-67.** Organoids were stained for the proliferation marker Ki-67 (red) and nuclear marker DAPI (blue). Tumor organoids display a high proportion of proliferating cells as well as normal organoids. Scale bar, 100μm.